co2amp

Misha Polyanskiy

2025-11-21

Contents

Chapter 1

General notes

1.1   Program capabilities

1. Ultrashort pulse amplification in CO_2 active medium

   - Rotational numbers $J = 0...79$
   - Regular, hot, and sequence bands
   - Isotopic CO_2

2. Molecular dynamics

   - Realistic pumping
   - Collisional relaxation processes
   - Stimulated transitions
   - Independent consideration of active medium regions at different elongations from the optical axis

3. Diffraction-based beam propagation

   - Beam manipulation with common optical elements
   - Arbitrary optical configurations

4. Linear dispersion and non-linear effects in optical materials

   - Pulse chirping
   - Kerr lensing
   - Self-phase modulation

5. Advanced optics

   - Chirped-pulse amplification
   - Spectral filtering
   - Trains of pulses
   - Staging (program output as an input for the next stage)

6. User's interface

   - Easy specification of parameters
   - Graphical output
   - Project save/recall

1.2 Availability, Tools, and Third Party Components

The simulation core **co2amp** and the user's interface shell **co2amp+** are written in the C++ programming language. **co2amp+** utilizes the `QT` library (`http://qt.io`), and `QT Creator`, a component of the `QT` project, is employed as the development environment. Windows executables are compiled using the `MinGW` compiler, which is part of the open-source `QT` distribution. The code is hosted on GitHub (`https://github.com/polyanskiy/co2amp`) and is freely available for use, modification, and redistribution under the GNU General Public License (GPL v.3) (`https://www.gnu.org/licenses/gpl-3.0.html`). A binary package is available as a Windows installer, containing pre-compiled executables, documentation, templates, and examples at `https://github.com/polyanskiy/co2amp/releases/`. The project leverages cross-platform libraries, facilitating compilation on other platforms (MacOS, Linux). **co2amp** relies on three third-party components: `gnuplot`, `7-zip`, and `HDF5`, available at `http://www.gnuplot.info/`, `https://www.7-zip.org/`, and `https://www.hdfgroup.org/solutions/hdf5/`, respectively. These components must be installed separately. The Windows installer is created using the `Nullsoft Scriptable Install System` (NSIS, `https://nsis.sourceforge.io/`), representing the only platform-specific component of the project. The documentation is primarily written in LaTeX(`http://www.latex-project.org`) using the `Overleaf` online editor and compiler (`https://www.overleaf.com/`). YAML and HDF5 file formats are adopted for specifying input parameters and storing output field information, respectively.

1.3 Acknowledgements

Viktor Platonenko from Moscow State University (Russia) provided a `Mathcad` code for pulse amplification in the CO_2 active medium, which served as the starting point for developing the **co2amp** program. Dr. Platonenko also offered valuable input during the early stages of the work on **co2amp**.

Chapter 2

Basic concepts

2.1 co2amp and co2amp+

co2amp is a terminal program designed for simulating the propagation of ultrashort pulses through an arbitrary cylindrically-symmetric optical system, which may include CO_2 amplifiers. It operates using inputs in the form of specially formatted text files and command line arguments, and generates outputs as tabulated data files and a binary file containing comprehensive information on the output field. While **co2amp** can function independently, its use is greatly facilitated by a graphical user interface, which significantly simplifies the management of the program's inputs and outputs.

    co2amp+ is a graphical user interface program that streamlines the process of handling multiple input and output files, as well as calculation parameters, by maintaining an organized and easily navigable working environment. **co2amp+** features functionality for saving and recalling the entire file structure of a project along with command line parameters in a single compressed '.co2' file.

2.2 Projects

The **co2amp** input parameters include the characteristics of the initial **pulse(s)**, the optical **layout** configuration, specifications for all **optics** used in the model (including laser amplifiers), and calculation parameters (e.g., calculation grid definition).

    The temporal shape of the pulse and the beam profile at every element of the optical layout are saved and can be accessed in both graphical and tabulated-numerical representations.

    All **co2amp** inputs and outputs for a certain model constitute a project.

    co2amp+ facilitates the storage of all inputs and outputs of the model, except for the output field, in a single compressed project file with a '.co2' extension. Complete pulse information (complex field at every node of the space-time calculation grid) at the system's output can be saved separately as a binary HDF5 file (with a '.pulse' extension) and used as an input for another project. An example of the input file structure of a '.co2' project accessed via the **co2amp+** interface is illustrated in Fig. 2.1.

2.3 Pulse, Layout and Optic

A **pulse** is a complex electric field defined at every node of the calculation grid. A project can include one or more input pulses. Each is defined in a separate YAML ('.yml') file. A pulse can be defined either by referencing an output from another project (a '.pulse' file) or by explicitly specifying the pulse's spatial and temporal profile.

    The optical **layout** consists of a series of infinitely-thin **optics** separated by free space. **Pulses** propagate freely between **optics**. A project must have exactly one **layout**. The **layout** is defined in a '.yml' file that
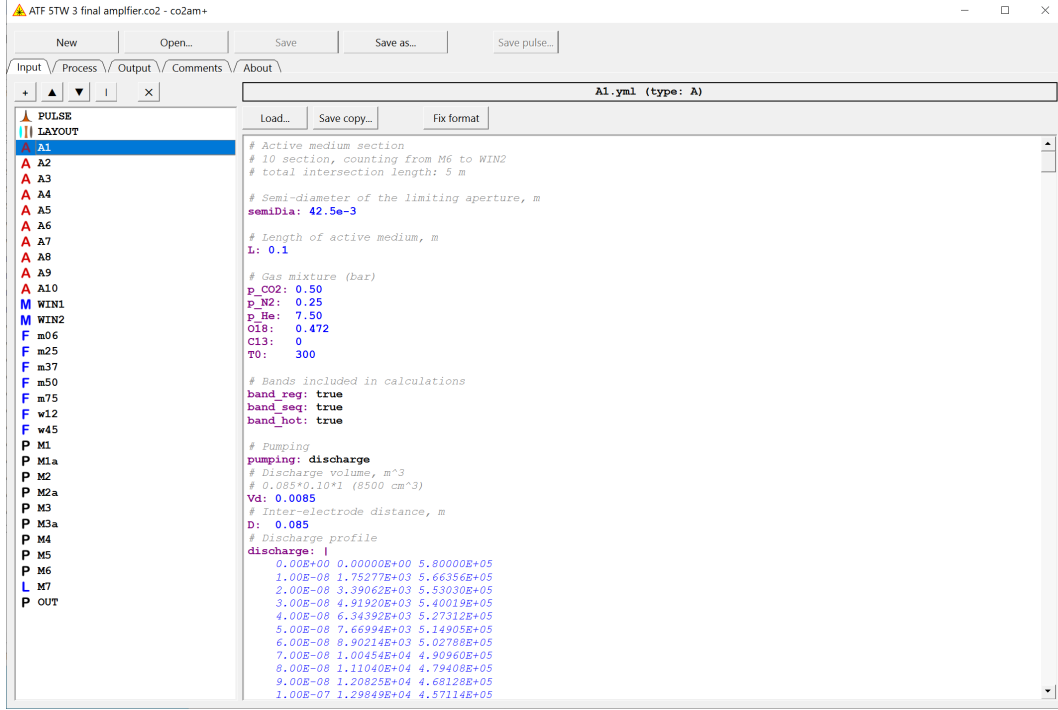
Figure 2.1: "Input" tab of the `co2amp+` user interface program. YAML files specifying the `pulse`, `layout`, and `optics` are listed on the left. Content of a selected file is displayed and can be edited in the big edit box on the right.

specifies the order of the `planes` and the distances between them.

An `optic` is a system element that alters the pulse as it passes through. Several types of `optics` are described in detail later. For example, a *Lens* is an `optic` introducing a radial-coordinate-dependent frequency shift, altering the beam's divergence. Each `optic` is specified in a separate '.yml' file. An `optic` can be used multiple times in the same `layout`, as in a laser cavity[1].

`co2amp` supports seven types of `optics`, listed in Table 2.1.

2.4   Calculation Grid

The `pulse` is defined as a complex electric field at the nodes of a 2-dimensional space-time calculation grid, which moves with the pulse. The calculation grid is primarily defined via `co2amp` command line arguments. The only exception is the maximum radial coordinate, equal to the semi-diameter of the clear aperture of an `optic`, and thus varies from one `optic` to another. The command line arguments associated with the pulse's space-time calculation grid include the numbers of nodes (representing "precision") in the time and radial coordinate grids, the minimum and maximum time limits, and the central frequency. The central frequency is essential for unambiguously defining the calculation grid in the frequency domain.

The pulse time frame is utilized for all `pulse`-related calculations (interaction with `optics`, free-space propagation) and for fast processes in some `optics`, such as fast molecular dynamics (stimulated transitions and rotational relaxation in an *Active Medium*). Processes significantly slower than the pulse duration (like the pumping of the active medium and vibrational relaxation) are modeled separately in a slower laboratory

---

[1]Internally, the `co2amp` code employs an additional concept: a `plane`. A `plane` is a `layout` element that, unlike an `optic`, appears in the `layout` only once. An `optic` is then associated with each `plane`. Essentially, a `plane` is a placeholder for an `optic`.

Table 2.1: Types of `Optics`

Type ID	Name	Description
A	*Active medium*	A CO_2 amplifier section.
P	*Probe*	A passive surface. May be used as a limiting aperture.
F	*Spatial filter*	An `optic` with coordinate-dependent transmission.
S	*Spectral filter*	An `optic` with frequency-dependent transmission.
L	*Lens*	An ideal thin lens.
M	*Material*	A layer of material. May introduce linear and/or non-linear dispersion and/or absorption.
C	*Chirper*	An `optic` that applies a chirp to the pulse. Typically a stretcher or compressor.

time-frame. The time-tick of this laboratory time-frame is also defined via a **co2amp** command line argument.

In **co2amp+**, the **co2amp** command line arguments are specified in the "Process" tab (Fig. 2.2). The number of nodes in both coordinates of the pulse space-time frame is always a power of two, enabling the use of Fast Fourier Transform (FFT) algorithms. Calculations with more nodes are generally more accurate but require longer computation times and more computer memory (both calculation time and required memory are approximately proportional to the product of the number of nodes in the time and space grids). Therefore, it is recommended to start the simulation with a smaller number of nodes and incrementally increase the grid density, repeating the simulation multiple times. The absence of significant changes in the program's output with an increase in the number of nodes indicates that the grid density is satisfactory.

The time-step, $\Delta t = (t_{\max} - t_{\min})/N_t$, where $t_{\max}$ and $t_{\min}$ define the time range and N_t is the number of nodes in the time grid, must be sufficiently small to accurately describe the pulse profile throughout its propagation in the optical system. It is also important to note that the time range and the number of nodes in the time grid define the frequency domain range and step: $\Delta\nu = 1/(t_{\max} - t_{\min})$ and $(\nu_{\max} - \nu_{\min}) = 1/\Delta t$. This means that the time range must be long enough to provide adequate resolution in the frequency domain, while the time step must be short enough to encompass the entire spectral region of interest.

Identifying an appropriate calculation grid is crucial for building an accurate model of an optical system. Investing effort in this part of the simulation process will yield fast and reliable calculations.

2.5 Units

SI units without prefixes, such as "meters, seconds, Amperes" (but not "centimeters, nanoseconds, kiloamperes"), are used in **co2amp** for input, output, and also internally within the code. **co2amp+** provides the functionality to change the units used for graphical representation of the calculation results on the "Output" tab (Fig. 2.3). However, when numerical data are accessed via [Right-click on a plot] – [Copy raw data], the units of the data are always in their "prefix-less" form.

2.6 Program Output

The output of the program includes the temporal and spatial structure of each `pulse` at every `optic` within the `layout`. Temporal (and spectral) profiles are integrated over the entire area of the `optic`, while spatial
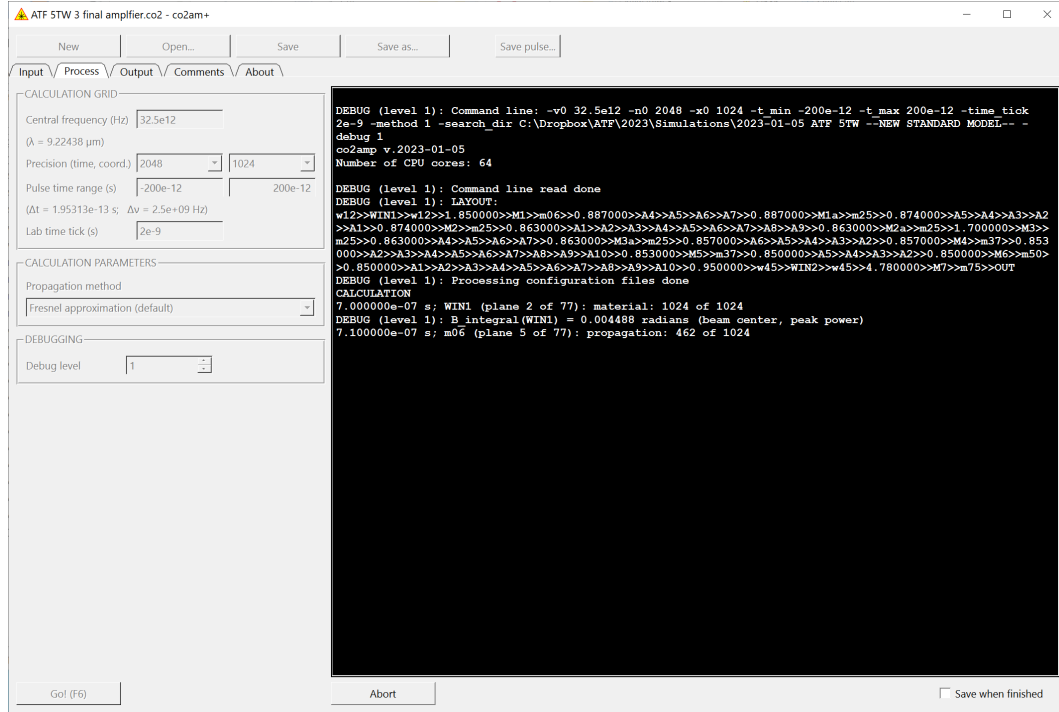
Figure 2.2: "Process" tab of the **co2amp+** user interface program. Values of **co2amp** command line arguments are specified on the left. **co2amp** output is displayed in the black text box on the right.

profiles are integrated over the duration of the pulse time-frame.

In the **co2amp+** "Output" tab, users can choose a `pulse` and an `optic` to display (Fig. 2.3). If the selected `optic` is utilized multiple times in the `layout`, there is also an option to specify which passes through the `optic` are to be displayed. Additionally, the integral pulse energy can be provided either at each pass through a selected `optic` or across all passes through all `optics` in the `layout`.

Output for certain types of `optics` includes additional type-specific information. For example, for an *Active medium*, this encompasses gain, discharge profile, population dynamics, and the dynamics of the distribution of pumping energy (fractions of discharge energy contributing to the excitation of laser levels, excitation of molecular translations, and ionization). Output for an `optic` of type *Probe* includes information on the phase of the optical field at the center of the beam.

2.7 "Comments" and "About" Tabs of **co2amp+**

The "Comments" tab in **co2amp+** provides an editable text box where users can enter any comments about the project. These comments will be stored as part of the project in the '.co2' file.

The "About" tab contains information about the versions of **co2amp** and **co2amp+**, including links to the license and the documentation (this file), author contact information, and a suggested citation format.
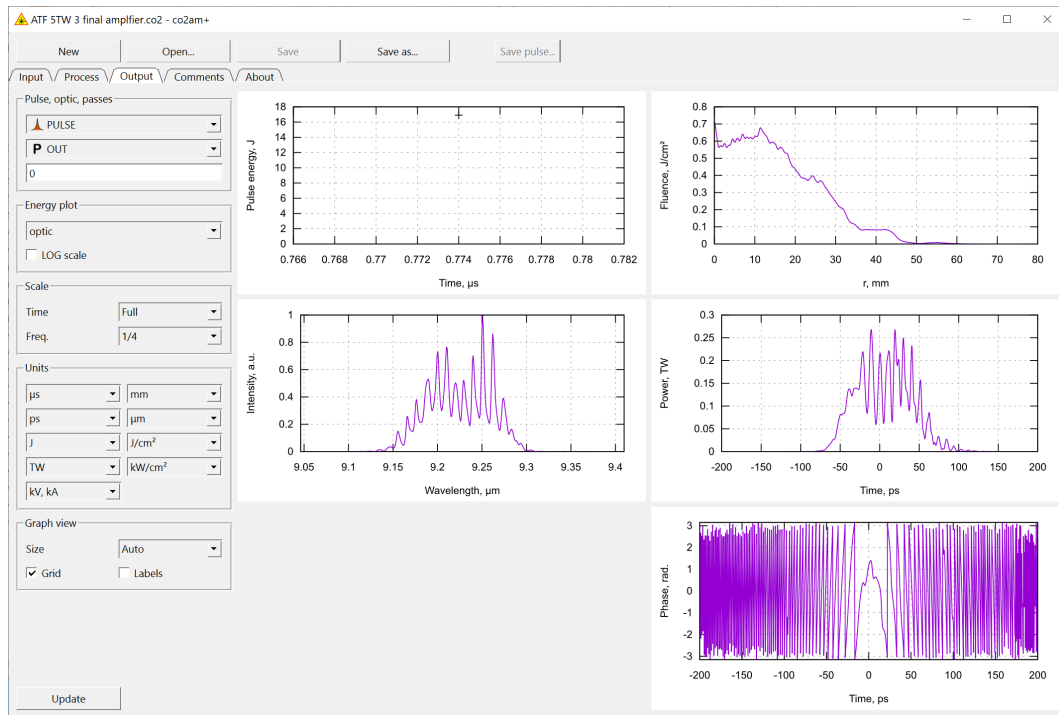
Figure 2.3: "Output" tab of the `co2amp+` user interface program. Controls on the left allow selecting the data to display and fine-tuning the look of the plots.

Chapter 3

Elements of a project

A project in **co2amp** must include the following elements, each specified in separate input YAML ('.yml') files:

1. One or more **pulses**

2. One or more **optics**

3. One **layout**

Each element is detailed in its dedicated YAML file[1]. The last **optic** in the **layout** must be of type P (*Probe*).

The subsequent sections provide brief descriptions of each of these elements and the models associated with them. For a comprehensive understanding, refer to the templates, example files, and the comments within them.

3.1 Pulse

Unless utilizing the output of another project (a '.pulse' file) as input, both the temporal and spatial shape of the input **pulse** must be defined in a corresponding YAML ('.yml') file. The **pulse** is assumed to be transform-limited, meaning it has no initial chirping. Specifications such as the **pulse** energy, central frequency, and injection time are also required. The injection time denotes the time-delay between the zero moment of the laboratory time frame ("slow" time frame) and the injection of a **pulse** into the optical system (the first **optic** in the **layout**). An example of a **pulse** configuration file is provided below.

```
#==========================
# PULSE.yml from 'examples/00 simple propagation.co2' project

t_in: 0
E: 1e-3
freq: 32.5e12

beam: GAUSS
w: 3e-3

pulse: GAUSS
fwhm: 2e-12
```

---

[1] **co2amp** additionally requires an input file 'config_files.yml' that enumerates all input YAML files and the types of corresponding elements. **co2amp+** automatically generates this file.

```
#=========================
```

This file specifies a 2 ps (FWHM) transform-limited Gaussian pulse with a $w = 3$ mm Gaussian beam profile, 1 mJ energy, and a 32.5 THz central frequency, injected into the system at $t_{\text{in}} = 0$. Several pre-defined beam and pulse profile options are available, such as `GAUSS`, `FLATTOP`, `SUPERGAUSS4`, `SUPERGAUSS6`, etc. Alternatively, a `FREEFORM` option allows for the specification of an arbitrary shape through a tabulated numerical profile (refer to the 'pulse.yml' template for details).

3.2 Layout

3.2.1 Configuration

The `layout` configuration defines the sequence of `optics` and the distances between them in the optical system. Below is an example of a simple `layout` configuration file:

```
#=========================
# LAYOUT.yml from 'examples/00 simple propagation.co2' project

- go: P1 >> 3 >> P2
  times: 1
#=========================
```

In this example, the system consists of two `optics`, `P1` and `P2`, separated by 3 meters of free space. The pulses pass through the system once. If the `times` value is greater than 1, a pulse after passing through `P2` will return to `P1`, and the propagation through the system will repeat for the specified number of times. A `layout` configuration file can contain several such "go-times" sequences. Below is an example of a `layout` configuration for a more complex system:

```
#=========================
# LAYOUT.yml from 'examples/ATF 5 TW/ATF 1 regen.co2' project

- go: str >> COU1
  times: 1

- go: 0.45 >> i >> 0.90 >> GE >> 0.25 >> w >> WIN1 >> w >> 0.45 >> AM1 >> 0.40 >> AM2 >> 0.45
>> w >> WIN2 >> w >> 0.10 >> MIR >> m >> 0.10 >> w >> WIN2 >> w >> 0.45 >> AM2 >> 0.40 >> AM1
>> 0.45 >> w >> WIN1 >> w >> 0.25 >> GE >> 0.90 >> i >> 0.45 >> COU2
  times: 15

- go: 0.45 >> i >> 0.90 >> GE >> 0.25 >> w >> WIN1 >> w >> 0.45 >> AM1 >> 0.40 >> AM2 >> 0.45
>> w >> WIN2 >> w >> 0.10 >> MIR >> m >> 0.10 >> w >> WIN2 >> w >> 0.45 >> AM2 >> 0.40 >> AM1
>> 0.45 >> w >> WIN1 >> w >> 0.25 >> OUT
  times: 1
#=========================
```

3.2.2 Dealing with Long Optical Elements

In the `co2amp` model, `optics` are considered infinitely thin. For long `optics`, such as an *Active Medium*, the model calculates the field modification accumulated by a `pulse` as it propagates through the `optic` and then applies this modification as if it occurred instantaneously. However, this approach might not be accurate if the actual optical element is lengthy and the `pulse` changes significantly while propagating through it, thereby interacting differently with various parts of the `optic`. The model's accuracy can be improved by dividing long elements into shorter sub-sections.

Fig. 3.1 illustrates an example of a 2-meter long `layout` with a meter-long active medium in the middle. In one scenario, shown in Fig. 3.1a, we first propagate the `pulse` to the midpoint of the amplifier section, then apply the amplification accumulated over 1 meter, and finally propagate the `pulse` to the last `optic`. The corresponding `layout` configuration is:
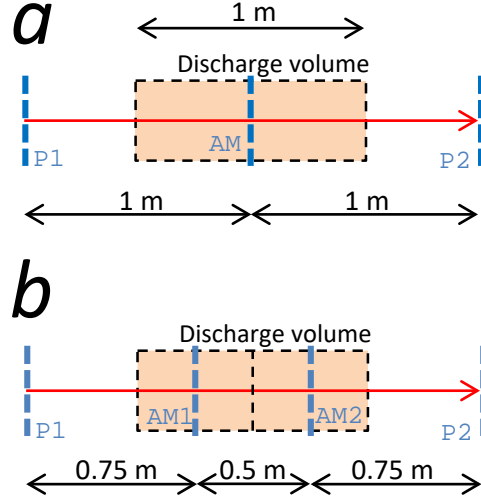
Figure 3.1: Example of `layout` configuration for a long `optic` (in this case, an *Active Medium*). a) The *Active Medium* is represented by a single `optic`. b) The *Active Medium* is split into two shorter sections.

```
#===========================
# long amplifier

- go: P1 >> 1 >> AM >> 1 >> P2
  times: 1
#===========================
```

Alternatively, the active medium can be represented by two 0.5-meter sections, as shown in Fig. 3.1b. The corresponding layout is:

```
#===========================
# long amplifier divided into two shorter sections

- go: P1 >> 0.75 >> AM1 >> 0.5 >> AM2 >> 0.75 >> P2
  times: 1
#===========================
```

By splitting a long amplifier into shorter sections, the population dynamics within each amplifier section is modeled more accurately, leading to a more realistic representation of the active medium.

3.2.3 Modeling of `Pulse` Propagation Between `Optics`

Consider free-space wave propagation between plane-parallel surfaces S' and S, separated by distance z, as illustrated in Fig. 3.2 for a system with cylindrical symmetry. According to the Huygens-Fresnel principle, the field E at a point on plane S is defined as a superposition of secondary waves emitted from every point

Figure 3.2: Application of the Huygens-Fresnel principle to beam propagation from plane S' to plane S in a system with cylindrical symmetry.

of plane S' [1]. This can be expressed in the case of cylindrical symmetry as [2, 3]:

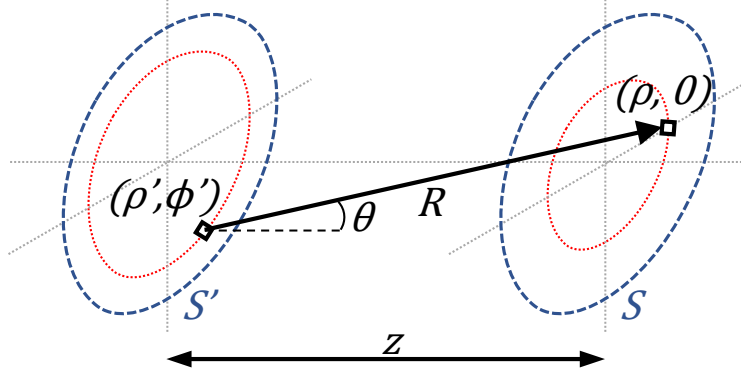$$E(\rho) = -\frac{i}{\lambda} \int_{\rho'=0}^{\infty} E'(\rho') \int_{\phi'=0}^{2\pi} \frac{e^{ikR}}{R} K d\phi' \rho' d\rho' \tag{3.1a}$$

$$R = \sqrt{\rho^2 + \rho'^2 + z^2 - 2\rho\rho' \cos\phi'} \tag{3.1b}$$

$$K = \cos\theta = \frac{z}{R} \tag{3.1c}$$

where λ is the wavelength, $k = 2\pi/\lambda$ the wavenumber, and K the obliquity factor as it appears in Rayleigh-Sommerfeld diffraction theory.

Since the field on the output plane S does not depend on the angular coordinate ϕ, $\phi = 0$ is chosen for the simplification of Eq. 3.1.

Direct numerical integration of Eq. 3.1, with $O(N^3)$ complexity, is very time-consuming. Therefore, an approximation is usually employed to accelerate computations. The most well-known approximation is Fresnel diffraction, which assumes:

$$K \approx 1$$
$$R \approx \begin{cases} z & \text{(denominator)} \\ z\left(1 + \frac{\rho^2 + \rho'^2 - 2\rho\rho'\cos\phi'}{2z^2}\right) & \text{(exponent)} \end{cases} \tag{3.2}$$

where "denominator" and "exponent" indicate the position of the R variable in Eq. 3.1a.

Substituting Eq. 3.2 into Eq. 3.1a and using the formula

$$\int_0^{2\pi} e^{\pm ia\cos\phi} d\phi = 2\pi J_0(a) \tag{3.3}$$

where J is the Bessel function, we obtain the expression for Fresnel diffraction with cylindrical symmetry:

$$E(\rho) \approx -\frac{2\pi i e^{ik\left(z + \frac{k\rho^2}{2z}\right)}}{\lambda z} \int_0^{\infty} E'(\rho') e^{i\frac{k\rho'^2}{2z}} J_0\left(\frac{k\rho\rho'}{z}\right) \rho' d\rho' \tag{3.4}$$

co2amp supports both Rayleigh-Sommerfeld (Eq. 3.1) and Fresnel (Eq. 3.4) based propagation methods. Users can also choose to ignore the **pulse** evolution during free-space propagation.

Eqs. 3.1 and 3.4 assume monochromatic light, which is not the case for ultrashort pulses that possess a non-negligible bandwidth. Therefore, in **co2amp**, propagation is calculated in the frequency domain: Eqs. 3.1 or 3.4 are applied to the Fourier-transformed field at each node of the frequency calculation grid. Afterward, an inverse Fourier transform is used to return to the time domain.

3.3 `Optic` Type A: *Active Medium*

The *Active Medium* is the most complex type of `optic` that can be utilized in a **co2amp** project. Detailed models used for simulating molecular dynamics and `pulse` amplification are described in a dedicated Chapter 4.

A configuration file for an `optic` of type A must include specifications of the gas mixture, pumping mechanism, and laser transitions considered in the simulations. An example of such a configuration file is provided below:

```
#=========================
# AM1.yml from 'examples/ATF 5 TW/ATF 3 final amplifier.co2' project

# Semi-diameter of the limiting aperture, m
semiDia: 45e-3

# Length of active medium, m
L: 0.57

# Gas mixture (bar)
p_CO2: 0.50
p_N2:  0.25
p_He:  7.50
O18:   0.472
C13:   0
T0:    300

# Bands included in calculations
band_reg: true
band_seq: true
band_hot: true

# Pumping
pumping: discharge
# Discharge volume, m^3
Vd: 0.0085
# Inter-electrode distance, m
D:  0.085
# Discharge profile
discharge: |
    0.00E+00 0.00000E+00 5.80000E+05
    1.00E-08 1.97186E+03 5.66356E+05
    2.00E-08 3.81445E+03 5.53030E+05
    3.00E-08 5.53410E+03 5.40019E+05
    4.00E-08 7.13691E+03 5.27312E+05
    ...
#=========================
```

The composition of the active medium, including isotopic enrichment of carbon dioxide, and the initial temperature are specified under the "Gas mixture (bar)" section.

For discharge pumping, the geometry of the discharge and its temporal profile are required. In the case of optical pumping, the wavelength, absorption cross-section, and the temporal profile of the pumping pulse must be provided.

The 'optic A (discharge pumped CO2 amplifier).yml' and 'optic A (optically pumped CO2 amplifier).yml' template files contain detailed information on the configuration file format and can be referred to for further guidance.

3.4 `Optic` Type P: *Probe*

A *Probe* is a passive type of `optic`. It does not alter the field that fits within its semi-diameter. This can be expressed mathematically as:

$$E(t, \rho) = E'(t, \rho) \tag{3.5}$$

where $E'(t, \rho)$ and $E(t, \rho)$ represent the field before and after passing through an `optic`, respectively.

However, a *Probe* `optic` can serve as a limiting aperture, exhibiting zero transmittance for $\rho >$ semiDia. The sole configuration parameter for an `optic` of type P is its semi-diameter. An example of a configuration file for a *Probe* with a 25 mm semi-diameter is shown below:

```
#=========================
# probe

semiDia: 25e-3
#=========================
```

3.5 `Optic` Type F: *Spatial Filter*

A *Spatial Filter* applies a specified coordinate-dependent transmittance function to a `pulse`:

$$E(t, \rho) = E'(t, \rho)\sqrt{\mathcal{T}(\rho)} \tag{3.6}$$

where $\mathcal{T}(\rho)$ is the transmittance function, as defined in the configuration file.

An example configuration for a *Spatial Filter* is shown below:

```
#=========================
# spatial filter

semiDia: 25e-3

filter: SIN
R: 10e-3
w: 10e-3
#=========================
```

For more details and configuration options, refer to the 'optic F (spatial filter).yml' template file.

3.6 `Optic Type S:` *Spectral Filter*

A *Spectral Filter* applies a specified frequency-dependent transmittance function to a `pulse`:

$$\widehat{E}'(\nu, \rho) = \mathcal{F}(E'(t, \rho))$$
$$\widehat{E}(\nu, \rho) = \widehat{E}'(\nu, \rho)\sqrt{\mathcal{T}(\nu)} \tag{3.7}$$
$$E(t, \rho) = \mathcal{F}^{-1}(\widehat{E}(\nu, \rho))$$

where $\mathcal{F}$ and $\mathcal{F}^{-1}$ denote the Fourier transform and the inverse Fourier transform, respectively, ν is the frequency, and $\mathcal{T}(\nu)$ is the transmittance function as defined in the configuration file.

An example configuration for a *Spectral Filter* is provided below:

```
#==========================
# spectral filter

semiDia: 25e-3

filter: FREEFORM
form: |
    32.0e12 1.0
    32.1e12 0.9
    32.2e12 0.7
    32.3e12 0.5
    32.4e12 0.3
    32.5e12 0.0
    32.6e12 0.3
    32.7e12 0.5
    32.8e12 0.7
    32.9e12 0.9
    33.0e12 1.0
#==========================
```

For further details and configuration options, refer to the 'optic S (spectral filter).yml' template file.

3.7 `Optic Type L:` *Lens*

A *Lens* functions as a standard optical lens within the system:

$$\widehat{E}'(\nu, \rho) = \mathcal{F}(E'(t, \rho))$$
$$\widehat{E}(\nu, \rho) = \widehat{E}'(\nu, \rho)\exp\left(-\frac{ik\rho^2}{2F}\right) \tag{3.8}$$
$$E(t, \rho) = \mathcal{F}^{-1}(\widehat{E}(\nu, \rho))$$

where $k = \frac{2\pi\nu}{c}$ is the wave number (c is the speed of light) and F is the focal length of the lens.

The calculation is performed in the frequency domain to ensure that the effective focal length remains consistent across all frequencies in the pulse spectrum.

An example configuration for a lens with a 1-meter focal length is shown below:

```
#==========================
# lens (F = 1 m)
```

```
semiDia: 25e-3

F: 1.0
#========================
```

3.8   `Optic Type M:` *Material*

In cases of oblique incidence, the effective intensity I_{eff} is reduced and the propagation distance in the material (effective thickness) Θ_{eff} is automatically adjusted based on the incidence angle θ_i and the refractive index n:

$$\theta_r = \arcsin\left(\frac{\sin\theta_i}{n_0}\right)$$

$$I_{\text{eff}} = I\frac{\cos\theta_i}{\cos\theta_r} \tag{3.9}$$

$$\Theta_{\text{eff}} = \frac{\Theta}{\cos\theta_r}$$

where I and Θ are the intensity before the `optic` and the actual thickness of the material, respectively, and θ_r is the refraction angle.

Linear Dispersion and Absorption

$$\widehat{E}'(\nu,\rho) = \mathcal{F}(E'(t,\rho))$$

$$\widehat{E}(\nu,\rho) = \widehat{E}'(\nu,\rho)\exp(i\Delta\phi)\sqrt{\exp(-\alpha_0\Theta_{\text{eff}})} \tag{3.10}$$

$$E(t,\rho) = \mathcal{F}^{-1}(\widehat{E}(\nu,\rho))$$

where the phase shift $\Delta\phi$ is defined as:

$$\Delta\phi = 2\pi\int_0^\nu (\nu'-\nu_c)\frac{dt}{d\nu'}d\nu', \tag{3.11}$$

$$\frac{dt}{d\nu'} = \frac{\Theta_{\text{eff}}}{c}\frac{dn_g}{d\nu'}, \tag{3.12}$$

with c as the speed of light, n_g as the group index of refraction, and ν_c as the central frequency. The dispersion formulas used for calculating n_g are given in Appendix C.

Nonlinear Interaction

$$E(t,\rho) = E'(t,\rho)\exp\left(2\pi i\nu_c\frac{\Theta_{\text{eff}}}{c}n_2 I_{\text{eff}}(t,\rho)\right)$$

$$I_{\text{eff}}(t,\rho) = 2h\nu_c(E'(t,\rho))^2\frac{\cos\theta_i}{\cos\theta_r} \tag{3.13}$$

where n_2 is the nonlinear refractive index, h is Planck's constant, and $I(t,r)$ is the field intensity. Numerical values of n_2 used in the program are given in Appendix C.

Configuration example for a *Material* `optic`:

```
#========================
# material

semiDia: 25e-3
```

```
material:  NaCl
thickness: 100e-3
tilt: 0
slices: 10
#========================
```

Currently supported materials include AgBr, AgCl, BaF$_2$, CdTe, CsI, GaAs, Ge, IRG22 (AMTIR1), IRG24, IRG25, KBr, KCl, KRS5, NaCl, NaF, Si, SiO$_2$, ZnS, ZnSe, and air. An arbitrary n_2 can be specified in the configuration file, with a predefined value used otherwise (see Appendix C). To enhance accuracy, the *Material* `optic` can be divided into several layers. A split-step method is employed for calculating linear and nonlinear interactions with a layer: first, a nonlinear interaction with a half-layer is calculated, followed by a full-layer linear interaction, and then a half-layer nonlinear interaction again.

3.9 `Optic Type C:` *Chirper*

A *Chirper* introduces a chirp to a pulse and is typically used to model a stretcher or compressor.

$$\widehat{E}'(\nu, \rho) = \mathcal{F}(E'(t, \rho))$$
$$\widehat{E}(\nu, \rho) = \widehat{E}'(\nu, \rho) \exp(i\Delta\phi) \tag{3.14}$$
$$E(t, \rho) = \mathcal{F}^{-1}(\widehat{E}(\nu, \rho))$$

where

$$\Delta\phi = 2\pi \int_0^\nu (\nu' - \nu_c) \frac{dt}{d\nu'} d\nu' \tag{3.15}$$

is the phase shift, ν_c is the central frequency, and $\frac{d\nu}{dt}$ is the chirp rate.

In the case of linear chirp, the chirp rate is constant, and Eq. 3.15 simplifies to:

$$\Delta\phi = 2\pi \int_0^\nu \frac{\nu' - \nu_c}{\mathcal{C}} d\nu' = \pi \frac{(\nu - \nu_c)^2}{\mathcal{C}}$$
$$\mathcal{C} = \frac{d\nu}{dt} \tag{3.16}$$

Positive chirp rate corresponds to a red chirp of the pulse.

An example configuration for a *Chirper* with linear chirp is shown below:

```
#========================
# stretcher (positive chirp <=> red chirp)

semiDia: 25e-3

chirp: LINEAR
c: 3.5e21
#========================
```

Chapter 4

Modeling of processes in CO_2 amplifiers

4.1 Basics of the molecular spectroscopy of CO_2

4.1.1 Isotopologues of CO_2 and their nomenclature

The **co2amp** model includes twelve isotopologues of CO_2 with different combinations of stable isotopes of carbon (^{12}C and ^{13}C) and oxygen (^{16}O, ^{17}O and ^{18}O). A commonly used three-digit notation designates the isotopologues of carbon dioxide, where each digit represents the isotope of an atom in the molecule in the order oxygen–carbon–oxygen, corresponding to the last digit of the isotope's mass number. In this notation, the digits *2* and *3* represent ^{12}C and ^{13}C, respectively, while the digits *6*, *7* and *8* represent ^{16}O, ^{17}O and ^{18}O, respectively. Thus, *626*, for instance, denotes a CO_2 molecule with the natural isotopic composition ^{16}O-^{12}C-^{16}O, and *638* stands for the ^{16}O-^{13}C-^{18}O isotopologue.

4.1.2 Vibrational levels of CO_2 molecule

Laser transitions

Laser transitions in CO_2 amplifiers occur between the rotational sub-levels of vibrational levels in the electronic ground state of the molecule. The primary laser transitions ("Regular bands") are between the first excited state of the antisymmetric stretching vibration and one of the combination vibrations involving the first excited state of the symmetric stretching and the second excited state of the bending vibration. However, transitions between higher energy levels are also possible, potentially contributing to the overall gain of the amplifier. Multiple vibrational energy levels are thus included in the **co2amp** amplification model. Figure 4.1 shows some of the laser transitions included in the **co2amp** amplification model and the vibrational levels involved in these transitions.

   Other vibrational levels contributing to the population dynamics of the laser levels are not shown in the figure but are included in the model as described in the following text. Additionally, the code includes experimental support for modeling laser transitions at approximately $4\,\mu m$ between the group of levels at the end of the sequence bands and the group of levels including the lower levels of the regular bands. Below, we describe the basics of the involved molecular spectroscopy, followed by the description of the model of the population dynamics and stimulated emission.

Vibrational level nomenclature

A standard scheme of vibrational level nomenclature uses the $\nu_1\,\nu_2^{l[e/f]}\,\nu_3$ notation, where ν_1, ν_2, and ν_3 are the numbers of quanta in the symmetric stretch, bending, and antisymmetric stretch vibrational modes,
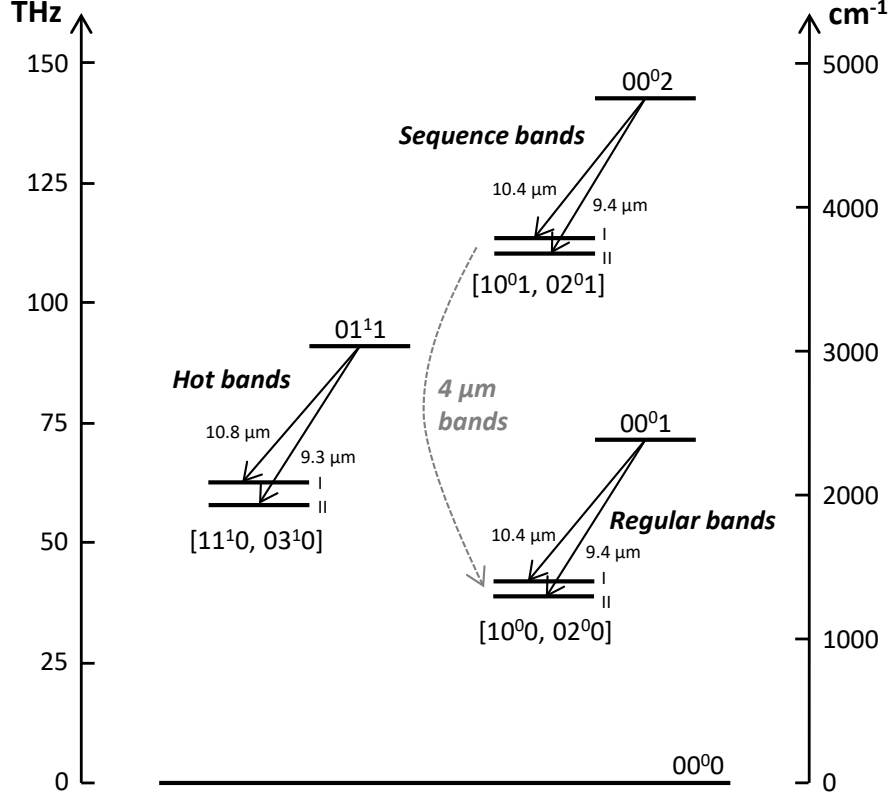
Figure 4.1: Vibrational transitions included in the amplification model. Wavelengths are given for natural CO_2 isotopologue (*626*).

respectively, and l is the vibrational angular momentum quantum number of the doubly degenerate bending vibration. States with $l \neq 0$ are further split into two sub-levels due to the two possible symmetries associated with the bending vibration. A letter e or f is added to the notation after the value of l to differentiate between these sub-levels.

In the CO_2 molecule, a strong Fermi coupling exists between the ν_1 and ν_2 vibrations, resulting in mixed states that cannot be directly attributed to a single set of vibrational quantum numbers. We refer to these levels by listing the contributing states in square brackets and adding a Roman numeral subscript indicating a sub-level number. For instance, the lower laser level of the 9.4 µm regular band is denoted as $[1\,0^0 0,\, 0\,2^0 0]_{\mathrm{II}}$.

In the HITRAN database, the symmetry of the bending vibration (e or f) is associated with the rotational levels rather than with the vibrational ones, as in the `co2amp` model. Associating the symmetry with the vibrational state makes modeling the energy distribution between ro-vibrational sub-levels more straightforward and transparent. Also, the letter e is associated with the $l = 0$ levels in HITRAN for database consistency.

Furthermore, in HITRAN, the mixed states are labeled by one of the contributing states followed by a sub-level number. The $[1\,0^0 0,\, 0\,2^0 0]_{\mathrm{II}}$ level, for example, is denoted as $1\,0^0 0\,(2)$ (or $1\,0\,0\,0\,2$ in the raw `.par` files). The letter e is then added to the rotational level labels (e.g., "P 20e").

Vibrational levels and transitions included in the `co2amp` model

Table 4.1 lists the vibrational levels included in the model. The levels in the table are grouped to include sub-levels arising from angular momentum splitting and Fermi coupling between the ν_1 and ν_2 vibrations.

Table 4.2 lists the supported transitions.

20

Table 4.1: Vibrational levels included in the model

#	Level	Parity	Weight	Description
		0 0 1 (Group 0)		
0	$0\,0^0 1$	u	1	Upper level of regular bands
		1 0 0 + 0 2 0 (Group 1)		
1	$[1\,0^0 0,\,0\,2^0 0]_I$	g	1/3	1, 2: lower levels of regular bands
2	$[1\,0^0 0,\,0\,2^0 0]_{II}$	g	1/3	1, 2, 3, 4: lower levels of 4 µm bands
3	$0\,2^{2e} 0$	g	1/6	
4	$0\,2^{2f} 0$	g	1/6	
		0 1 1 (Group 2)		
5	$0\,1^{1e} 1$	g	1/2	Upper levels of hot bands
6	$0\,1^{1f} 1$	g	1/2	
		1 1 0 + 0 3 0 (Group 3)		
7	$[1\,1^{1e} 0,\,0\,3^{1e} 0]_I$	u	3/16	7, 8, 9, 10: lower levels of hot bands
8	$[1\,1^{1e} 0,\,0\,3^{1e} 0]_{II}$	u	3/16	
9	$[1\,1^{1f} 0,\,0\,3^{1f} 0]_I$	u	3/16	
10	$[1\,1^{1f} 0,\,0\,3^{1f} 0]_{II}$	u	3/16	
11	$0\,3^{3e} 0$	u	1/8	11, 12: not currently included in the
12	$0\,3^{3f} 0$	u	1/8	amplification model
		0 0 2 (Group 4)		
13	$0\,0^0 2$	g	1	Upper level of sequence bands
		1 0 1 + 0 2 1 (Group 5)		
14	$[1\,0^0 1,\,0\,2^0 1]_I$	u	1/3	14, 15: lower levels of sequence bands
15	$[1\,0^0 1,\,0\,2^0 1]_{II}$	u	1/3	14, 15, 16, 17: upper levels of 4 µm bands
16	$0\,2^{2e} 1$	u	1/6	
17	$0\,2^{2f} 1$	u	1/6	
		0 1 2 (Group 6) Reserved for future use		
		1 1 1 + 0 3 1 (Group 7) Reserved for future use		
		0 0 3 (Group 8) Reserved for future use		
		1 0 2 + 0 2 2 (Group 9) Reserved for future use		

Please note that support for the 4-µm transitions is experimental and is not included in the calculations by default. To enable these transitions, use the `band_4um: true` instruction in the configuration of the active medium. It is also recommended to disable other transitions when enabling this feature.

Table 4.2: Supported vibrational transitions

Band #	Transition
Regular bands	
0	$00^01 \rightarrow [10^00, 02^00]_I$
1	$00^01 \rightarrow [10^00, 02^00]_{II}$
Hot bands	
2e	$01^{1e}1 \rightarrow [11^{1e}0, 03^{1e}0]_I$
2f	$01^{1f}1 \rightarrow [11^{1f}0, 03^{1f}0]_I$
3e	$01^{1e}1 \rightarrow [11^{1e}0, 03^{1e}0]_{II}$
3f	$01^{1f}1 \rightarrow [11^{1e}0, 03^{1f}0]_{II}$
Sequence bands	
4	$00^02 \rightarrow [10^01, 02^01]_I$
5	$00^02 \rightarrow [10^01, 02^01]_{II}$
4-μm bands	
6	$[10^01, 02^01]_I \rightarrow [10^00, 02^00]_I$
7	$[10^01, 02^01]_{II} \rightarrow [10^00, 02^00]_{II}$
8e	$02^{2e}1 \rightarrow 02^{2e}0$
8f	$02^{2f}1 \rightarrow 02^{2f}0$

Statistical weights of vibrational levels

We assume a simple statistical distribution of the population among the levels in each group to assign a weight coefficient to each level. To demonstrate the procedure for calculating the weights, let's consider the Group 1 including levels #1, #2, #3, and #4.

We start from the normal mode populations; there are two modes involved:

- The mode $1\,0\,0$ contains half of the population (weight coefficient $\frac{1}{2}$) and has no splitting due to angular momentum, as the degenerate vibration ν_2 is not involved. The only sub-level is thus $1\,0^00$.

- The mode $0\,2\,0$ contains the other half of the population (weight coefficient $\frac{1}{2}$) and is split due to angular momentum into three sub-levels: $0\,2^00$, $0\,2^{2e}0$, and $0\,2^{2f}0$. Each sub-level of $0\,2\,0$ thus has a weight coefficient of $\frac{1}{6}$ (since $\frac{1}{2}$ divided equally among three sub-levels).

Since $1\,0^00$ and $0\,2^00$ are coupled through Fermi resonance, their populations are assumed to redistribute equally between the resultant mixed levels (levels #1 and #2). Therefore, the weight coefficient for each mixed level is calculated as:

$$\frac{\text{Weight from } 1\,0^00 + \text{Weight from } 0\,2^00}{2} = \frac{\frac{1}{2} + \frac{1}{6}}{2} = \frac{1}{3}.$$

Thus, each mixed level (#1 and #2) receives a weight coefficient of $\frac{1}{3}$.

The sub-levels resulting from the angular momentum splitting of $0\,2\,0$, namely $0\,2^{2e}0$ (level #3) and $0\,2^{2f}0$ (level #4), retain their individual weight coefficients of $\frac{1}{6}$ each.

This approach ensures that the total population is conserved, and the weights assigned to each sub-level reflect the statistical distribution due to the coupling and splitting mechanisms.

4.1.3 Rotational sub-levels

Rotational sub-level population in the rotational equilibrium is calculated as

$$N^0_{rot}(J) = z(J) \times s(J) \times N_{vib}. \tag{4.1}$$

Here, N_{vib} is the total population density of the corresponding vibrational level.

$z(J)$ is the rotational Boltzmann distribution function defined by:

$$z(J) = \frac{hB}{kT}(2J+1)\exp\left(-\frac{hB}{kT}J(J+1)\right) \tag{4.2}$$

where B is the rotational constant, $h = 6.626\,069\,57 \times 10^{-34}\,\mathrm{J\,s}$, and $k = 1.380\,648\,8 \times 10^{-23}\,\mathrm{J\,K^{-1}}$.

To determine the coefficient $s(J)$, follow these steps:

- If $J < l$:
$$s(J) = 0$$

- If $J \geq l$:

    - For symmetric isotopologues (626, 727, 636, 828, 737, and 838):
        * If parity $= g$ and symmetry $= e$ or   parity $= u$ and symmetry $= f$
        $$s(J) = \begin{cases} 2 & \text{for even } J \\ 0 & \text{for odd } J \end{cases}$$

        * If parity $= g$ and symmetry $= f$ or   parity $= u$ and symmetry $= e$
        $$s(J) = \begin{cases} 0 & \text{for even } J \\ 2 & \text{for odd } J \end{cases}$$

    - For asymmetric isotopologues (627, 628, 728, 637, 638, and 738):
    $$s(J) = 1$$

In the above:

- l is the vibrational angular momentum. Rotational levels with $J < l$ are not populated due to angular momentum coupling restrictions.

- The **parity** of the vibrational state is determined by the sum of quanta in the ungerade (u) vibrational modes (v_2 and v_3):
$$\text{parity} = \begin{cases} g & \text{if } v_2 + v_3 \text{ is even} \\ u & \text{if } v_2 + v_3 \text{ is odd} \end{cases}$$

- The **symmetry** refers to the e/f symmetry labels of the rotational-vibrational levels, which are determined by the coupling of rotational angular momentum J and vibrational angular momentum l. The e/f labels are adapted from the HITRAN database.

- For symmetric isotopologues, the statistical weight $s(J)$ is 2 for allowed rotational levels due to nuclear spin statistical weights, and 0 for forbidden levels.

- For asymmetric isotopologues, there are no symmetry restrictions due to the lack of identical nuclei, so all rotational levels with $J \geq l$ are populated, and $s(J) = 1$.

4.1.4 Use of HITRAN Data

Data for the supported transitions are extracted from the HITRAN database [4]. These data include transition frequencies (ν), Einstein coefficients (A), and the rotational quantum numbers of the upper and lower laser levels (J_U and J_L, respectively) for each ro-vibrational transition. The molecular constants, particularly the rotational constant B used in Eq. 4.2, for each vibrational level included in the model, are determined by fitting the HITRAN data as described in Appendix B.

Because not all transitions that could influence amplification are included in HITRAN for all isotopologues, additional transitions are, in some cases, included by calculating their frequencies using the fitted molecular constants and assigning them realistic Einstein coefficients. These coefficients are estimated by assuming that all coefficients in a given vibrational transition are equal for all rotational lines. If no rotational line for a vibrational transition is listed, an educated guess is made based on the A values of other bands and isotopologues. Additional `.par` files, containing only the information needed for calculations, are generated to list these estimated transitions and are included with the `co2amp` distribution.

Transitions derived from the original HITRAN data and additional estimated transitions included in separate `.par` files are detailed in Appendix B.

Note that all `.par` files in the `hitran_data` folder are scanned for supported transitions, and all matches are included in the calculations. It is therefore important to ensure that transitions are not duplicated across different files.

4.2 Molecular dynamics

4.2.1 Time frames

Two time frames are employed in the `co2amp` models to simulate processes that typically occur at rates differing by orders of magnitude:

- **Lab time frame:** This time frame is used to describe relatively slow processes, such as the dynamics of active medium pumping and vibrational relaxation. A typical time step for the lab time frame is on the order of a nanosecond.

- **Pulse time frame:** This is a fast time frame that moves with the laser pulse. It forms part of the spatio-temporal calculation grid used to represent the pulse. The temporal grid must be sufficiently dense to accurately capture the pulse's temporal structure and wide enough to ensure an appropriate spectral resolution. Processes such as pulse amplification and rotational relaxation are computed within the pulse time frame.

4.2.2 Temperature model

A 3-temperature model is used to describe the vibrational dynamics of the active medium in CO_2 amplifiers. In this model, the following temperatures represent the distribution of energy among molecular vibrations:

- T_2: Vibrational temperature of the ν_1 and ν_2 modes of CO_2.

- T_3: Vibrational temperature of the ν_3 mode of CO_2.

- T_4: Vibrational temperature of N_2.

The temperature model adopted in `co2amp` relates the average number of quanta in each vibrational mode of the CO_2 molecule to a mode temperature, as described by the first two equations in 4.3. The temperatures of the ν_1 and ν_2 modes, coupled by Fermi resonance, are considered equal, and thus only T_2 is used to describe both modes.

Vibrational temperatures are related to the average number of quanta e_x in the corresponding vibrations as follows:

$$e_2 = \frac{2}{\exp\left(\frac{960}{T_2}\right) - 1},$$

$$e_3 = \frac{1}{\exp\left(\frac{3380}{T_3}\right) - 1}, \tag{4.3}$$

$$e_4 = \frac{1}{\exp\left(\frac{3350}{T_4}\right) - 1}.$$

The factor of 2 in the first equation accounts for the two-fold degeneracy of the energy levels of the bending vibration.

In thermal equilibrium, the vibrational energy distribution follows the Boltzmann distribution. For the groups of vibrational levels defined in Table 4.1, this distribution is expressed as:

$$N_{001} = \frac{N}{\mathcal{Q}} \exp\left(-\frac{3380}{T_3}\right),$$

$$N_{100+020} = 2\frac{N}{\mathcal{Q}} \exp\left(-\frac{2 \times 960}{T_2}\right),$$

$$N_{011} = \frac{N}{\mathcal{Q}} \exp\left(-\frac{960}{T_2}\right) \exp\left(-\frac{3380}{T_3}\right),$$

$$N_{110+030} = 2\frac{N}{\mathcal{Q}} \exp\left(-\frac{3 \times 960}{T_2}\right),$$

$$N_{002} = \frac{N}{\mathcal{Q}} \exp\left(-\frac{2 \times 3380}{T_3}\right),$$

$$N_{101+021} = 2\frac{N}{\mathcal{Q}} \exp\left(-\frac{2 \times 960}{T_2}\right) \exp\left(-\frac{3380}{T_3}\right), \tag{4.4}$$

$$N_{012} = \frac{N}{\mathcal{Q}} \exp\left(-\frac{960}{T_2}\right) \exp\left(-\frac{2 \times 3380}{T_3}\right),$$

$$N_{111+031} = 2\frac{N}{\mathcal{Q}} \exp\left(-\frac{3 \times 960}{T_2}\right) \exp\left(-\frac{3380}{T_3}\right),$$

$$N_{003} = \frac{N}{\mathcal{Q}} \exp\left(-\frac{3 \times 3380}{T_3}\right),$$

$$N_{102+022} = 2\frac{N}{\mathcal{Q}} \exp\left(-\frac{2 \times 960}{T_2}\right) \exp\left(-\frac{2 \times 3380}{T_3}\right).$$

Here, N is the density of CO_2 molecules, and $\mathcal{Q}$ is the partition function [5]:

$$\frac{1}{\mathcal{Q}} = \left(1 - \exp\left(-\frac{1920}{T_2}\right)\right) \cdot \left(1 - \exp\left(-\frac{3380}{T_3}\right)\right) \cdot \left(1 - \exp\left(-\frac{960}{T_2}\right)\right)^2. \tag{4.5}$$

The intra-mode vibrational energy thermalization process is typically very fast. However, if the partial pressure of CO_2 is very low, or if the active medium is pumped by a very short optical pulse, the finite thermalization time must be considered. The thermalization time, τ_V, is assumed to be the same for all vibrational modes and is adopted from [6], where the relaxation time of the (10^01) and (02^01) levels is given as:

$$\tau_V \ [\text{s}] = \frac{10^{-6}}{750 \left(3.9 \, P_{CO_2}\right)}, \tag{4.6}$$

where the pressure P_{CO_2} is measured in bar. Note that since intra-mode vibrational energy thermalization only involves collisional energy transfer between CO_2 molecules, the thermalization time does not depend on the partial pressures of other gases, such as He and N_2.

During pumping and amplification, the populations of vibrational levels are treated independently for each CO_2 isotopologue. Thermalization is then accounted for on the "slow" lab time frame. Due to the lack of data on inter-isotopologue vibrational energy transfer rates and to simplify calculations, the same relaxation time, τ_V, is used for both inter-mode and intra-isotopologue thermalization.

It is assumed that the vibrational temperatures T_2 and T_3 are identical for all CO_2 isotopologues. This assumption is justified by the small energy mismatch between vibrational levels of different isotopic species, allowing rapid inter-molecular V-V energy exchange.

In the `co2amp` model, pumping and vibrational relaxation processes are slow compared to the duration of the laser pulse. Therefore, only stimulated transitions contribute to population changes during the pulse.

Rotational sub-level populations are also subject to thermalization. However, the corresponding thermalization time, τ_R, depends on collisions with all components of the active medium, not just CO_2. This time can be fast and comparable to the pulse duration, so τ_R is included in the pulse time frame calculations modeling pulse amplification, as described Section 4.3

4.2.3 Pumping by electric discharge

Simulations of active medium pumping by electric discharge are conducted following the approach described by Karlov and Konev [7].

Pumping is modeled using the Boltzmann equation in the following form [8, 9]:

$$
-\frac{1}{3}\left(\frac{\mathcal{E}}{\mathcal{N}}\right)^2 \frac{d}{du}\left[u\left(\sum_j y_j Q_{mj}(u)\right)^{-1}\frac{df(u)}{du}\right] =
$$

$$
1.09 \times 10^{-3}\frac{d}{du}\left[u^2 f(u)\sum_j \frac{y_j}{M_j}Q_{mj}(u)\right] \quad + \quad \sum_{j=1,2} y_j C_j \frac{d}{du}(uf(u)) \quad + \quad 6By_2\frac{d}{du}(uQ(u)f)
$$

$$
+ \quad \sum_j y_j \sum_k (u+u_{jk})Q_{jk}(u+u_{jk})f(u+u_{jk}) \quad - \quad uf(u)\sum_j y_j \sum_k Q_{jk}(u) \tag{4.7}
$$

where the terms represent the following:

- The left-hand side describes the energy of electrons in the electric field.

- The first term on the right-hand side represents energy transfer via elastic collisions between electrons and molecules.

- The second and third terms describe collisions involving rotational excitation of molecules.

- The last two terms account for inelastic collisions that transfer energy u_{jk} into vibrational and electronic excitations, as well as ionization.

Here:

- Electron energy u is expressed in electronvolts (eV).

- The ratio of the electric field to the full molecular density, $\mathcal{E}/\mathcal{N}$, is expressed in units of 10^{-16} V $\cdot$ cm^2.

- y_j are the relative molecule concentrations ($j = 1$ corresponds to CO_2, $j = 2$ to N_2 and $j = 3$ to He);

- $M_1 = 44$, $M_2 = 28$, $M_3 = 4$ are the molar masses;

- $C_1 = 8.2 \times 10^{-4}$ eV $\cdot$ Å^2 [10];

- $C_2 = 5.06 \times 10^{-4}$ eV $\cdot$ Å^2 [11];

- $B = 2.5 \times 10^{-4}$ eV is the N_2 rotational constant.

- Numerical values of the cross-sections Q and the transferred energies u_{jk} are summarized in Appendix A

Equation 4.7 is solved numerically using the tridiagonal matrix algorithm. Distribution function $f(u)$ is then used in the following calculations.

The rate constant ω_{jk}, and the electron drift speeds v_d are defined as:

$$\omega_{jk}\left[\frac{cm^3}{s}\right] = 5.93 \times 10^{-9} \int_0^\infty u Q_{jk}(u) f(u) du \tag{4.8}$$

$$v_d\left[\frac{cm}{s}\right] = -5.93 \times 10^7 \left(\frac{1}{3}\frac{\mathcal{E}}{\mathcal{N}}\right)\frac{df(u)}{du}\int_0^\infty u \left(\sum_j y_j Q_{mj}(u)\right)^{-1} du \tag{4.9}$$

The fraction of electron energy transmitted via inelastic processes is defined as

$$z_{jk} = 10^{16}\frac{y_j u_{jk}\omega_{jk}}{\left(\frac{\mathcal{E}}{\mathcal{N}}\right)v_d} \tag{4.10}$$

The fraction of electron energy transmitted to translations and rotations are the following:

$$z_t = 5.93 \times 10^7 \frac{1.09 \times 10^{-3}\int_0^\infty u^2\left(\sum_j \frac{y_j}{M_j}Q_{mj}(u)\right)f(u)du}{\left(\frac{\mathcal{E}}{\mathcal{N}}\right)v_d} \tag{4.11}$$

$$z_r = 5.93 \times 10^7 \frac{\sum_{j=1,2} y_j C_j \int_0^\infty u f(u)du + 6y_2 B\int_0^\infty u Q(u)f(u)du}{\left(\frac{\mathcal{E}}{\mathcal{N}}\right)v_d} \tag{4.12}$$

The distribution of the excitation energy is calculated using the following expressions:

$q_2 = \sum_{k=1}^{6} z_{1k}$ - fraction of energy transferred to CO_2 symmetric stretch (ν_1) and bending (ν_2) modes;

$q_3 = z_{17}$ - fraction of energy transferred to CO_2 asymmetric stretch mode (ν_3);

$q_4 = \sum_{k=1}^{8} z_{2k}$ - fraction of energy transferred to N_2 vibrations;

$q_T = z_t + z_r$ - fraction of energy transferred to translation and rotation;

$q_{ei} = \sum_{k=9}^{15} z_{2k} + \sum_{k=8}^{10} z_{1k}$ - fraction of energy spent on excitation of electronic levels and ionization.

Finally, we can calculate the pumping rates for each of the vibrational modes considered in the model:

$$p_{e4} = 0.8 \times 10^{-3}\frac{q_4}{ny_2}W(t),$$
$$p_{e3} = 0.8 \times 10^{-3}\frac{q_3}{ny_1}W(t), \tag{4.13}$$
$$p_{e2} = 2.8 \times 10^{-3}\frac{q_2}{ny_1}W(t),$$

where $W(t)$ is the discharge power density measured in kW/cm^3 and $n = 273\frac{p[bar]}{T_0[K]}$ is the total concentration of gas molecules in the active medium.

4.2.4 Optical Pumping

For optical pumping, the pumping rates are calculated using the following expressions:

$$p_{e4} = 0,$$

$$p_{e3} = \begin{cases} \Phi\sigma & \text{direct excitation of } (00^01) \text{ at } \sim 4.3 \ \mu\text{m}, \\ \Phi\sigma & \text{excitation via } (10^01, 02^01) \text{ at } \sim 2.8 \ \mu\text{m}, \\ \Phi\sigma & \text{excitation via } (20^01, 12^01, 04^01) \text{ at } \sim 2.0 \ \mu\text{m}, \\ 2\Phi\sigma & \text{excitation via } (00^02) \text{ at } \sim 2.2 \ \mu\text{m}, \\ 3\Phi\sigma & \text{excitation via } (00^03) \text{ at } \sim 1.4 \ \mu\text{m}. \end{cases}$$

$$p_{e2} = \begin{cases} 0 & \text{direct excitation of } (00^01) \text{ at } \sim 4.3 \ \mu\text{m}, \\ 2\Phi\sigma & \text{excitation via } (10^01, 02^01) \text{ at } \sim 2.8 \ \mu\text{m}, \\ 4\Phi\sigma & \text{excitation via } (20^01, 12^01, 04^01) \text{ at } \sim 2.0 \ \mu\text{m}, \\ 0 & \text{excitation via } (00^02) \text{ at } \sim 2.2 \ \mu\text{m}, \\ 0 & \text{excitation via } (00^03) \text{ at } \sim 1.4 \ \mu\text{m}. \end{cases}$$

(4.14)

Here, Φ is the flux of the pumping photons (number of photons per m^2 per second), and σ is the absorption cross-section.

Equation 4.14 indicates that each pumping photon delivers one quantum of energy to the upper laser level, and either zero, two, or four quanta to the lower level, depending on the pumping transition.

4.2.5 Pumping and vibrational relaxation dynamics

The dynamics of pumping and vibrational relaxation are modeled in the lab time frame and are described by the following equations:

$$\frac{de_4}{dt} = p_{e4} - r_a(e_4 - e_3),$$

$$\frac{de_3}{dt} = p_{e3} + r_c(e_4 - e_3) - r_3 f_3,$$

$$\frac{de_2}{dt} = f_2 \left(p_{e2} + 3r_3 f_3 - r_2(e_2 - e_{2T}) \right),$$

(4.15)

where

$$f_2 = \frac{2(1 + e_2)^2}{2 + 6e_2 + 3e_2{}^2}; \quad f_3 = e_3(1 + e_2/2)^3 - (1 + e_3)(e_2/2)^3 \exp(-500/T);$$

$$r_a = kn y_1; \quad r_c = kn y_2; \quad r_2 = k_2 n; \quad r_3 = k_3 n;$$

$$k_2 = \sum_{i=1}^{3} y_i k_{2i}; \quad k_3 = \sum_{i=1}^{3} y_i k_{3i};$$

$$e_{2T} = \frac{2}{\exp(960/T) - 1}$$

(4.16)

Here, p_e is measured in μs^{-1}, and the constants k are calculated using the following expressions [12, 13]:

$$k = 240/T^{1/2};$$
$$k_{31} = A(t)\exp(4.138 + 7.945x - 631.24x^2 + 2239x^3);$$
$$k_{32} = A(t)\exp(-1.863 + 213.3x - 2796.2x^2 + 9001.9x^3);$$
$$k_{33} = A(t)\exp(-3.276 + 291.4x - 3831.8x^2 + 12688x^3); \tag{4.17}$$
$$k_{21} = 1.16 \times 10^3 \exp(-59.3x);$$
$$k_{22} = 8.55 \times 10^2 \exp(-69x);$$
$$k_{23} = 1.3 \times 10^3 \exp(-40.6x)$$

where $x = T^{-1/3}$, $A(t) = (T/273)(1 + e_{2T}/2)^{-3}$, and the temperature T is expressed in kelvins (K).
Finally, the dynamics of the gas temperature are described by the following equation:

$$\frac{dT}{dt} = \frac{y_1}{C_V}(500r_3f_3 + 960r_2(e_2 - e_{2T})) + 2.7\frac{W(t)q_T}{nC_V}, \tag{4.18}$$

where $C_V = 2.5(y_1 + y_2) + 1.5y_3$.

4.3 Amplification

Amplification is simulated in the pulse time frame using the following equations, which also account for rotational relaxation [14, 15]:

$$\frac{\partial E}{\partial z} = -\sum_j \rho_j,$$
$$\frac{\partial \rho_j}{\partial t} + \left(2\pi i(\nu_c - \nu_{0j}) + \frac{1}{\tau_2}\right)\rho_j = -\frac{\sigma_j n_j E}{2\tau_2}, \tag{4.19}$$
$$\frac{\partial n_j}{\partial t} + \frac{n_j - n_j^0}{\tau_R} = 4(\rho_j E^* + c.c.),$$

where summation is done over all rotational-vibrational transitions of all CO_2 isotopologues, and
E - complex field envelope,
ρ_j - polarization of the medium,
z - linear coordinate along the direction of beam propagation,
t - time,
n_j - population inversion of the transition (difference of population densities of upper and lower levels),
n_j^0 - equilibrium population inversion of the transition,
ν_c - carrier frequency,
ν_{0j} - transition frequency in the line center,
σ_j - transition cross-section in the line center,
τ_2 - polarization dephasing time,
τ_R - rotational relaxation time.
The line-center cross-section is calculated using the expression [16]:

$$\sigma_j \ [\text{m}^2] = \frac{(\lambda_j \ [\text{m}])^2 A_j \ [\text{s}^{-1}]}{4} \times \frac{\tau_2 \ [\text{s}]}{\pi}. \tag{4.20}$$

Here, the first term represents the integrated cross-section of the rotational line, and the second term gives the maximum of the normalized Lorentzian profile of a line with a half-width at half-maximum (HWHM) of $\Delta\nu_{\text{HWHM}} = 1/(2\pi\tau_2)$.
Optical intensity I is related to the field amplitude as follows:

$$I[\text{W/m}^2] = 2h[\text{J} \cdot \text{s}]\nu_c[\text{s}^{-1}]|E|^2 \tag{4.21}$$

Dephasing and relaxation times are defined by the following equations:

$$\tau_2[\text{s}] = \frac{10^{-6}}{\pi \times 7.61 \times 750 \times (P_{CO2} + 0.73 P_{N2} + 0.64 P_{He})},$$

$$\tau_R[\text{s}] = \frac{10^{-7}}{750 \times (1.3 P_{CO2} + 1.2 P_{N2} + 0.6 P_{He})},$$

(4.22)

where pressure P is measured in bars.

The change in population due to stimulated transitions is calculated for each vibrational level of each isotopologue using the last equation from Equations (4.19):

$$\frac{d}{dt} N_U = 2 \sum_j \left(\rho_J E^* + \text{c.c.} \right),$$

$$\frac{d}{dt} N_L = -2 \sum_j \left(\rho_J E^* + \text{c.c.} \right),$$

(4.23)

where the summation is over all rotational transitions originating from (N_U) or ending at (N_L) the corresponding vibrational level.

In the next step, we calculate the overall change in the ν_2 and ν_3 quanta, denoted as ΔN_{ν_2} and ΔN_{ν_3}, respectively. This is done by summing the population changes of all levels for all isotopologues, multiplying each by the number of corresponding quanta in the given level. In this calculation, we consider each ν_1 quantum as equivalent to two ν_2 quanta, an approximation based on the assumption of equal T_1 and T_2 temperatures due to Fermi coupling.

The changes in the average quantum numbers in the vibrational modes due to stimulated transitions are calculated as follows:

$$\Delta e_3 = \frac{\Delta N_{\nu_3}}{N},$$

$$\Delta e_2 = \frac{\Delta N_{\nu_2}}{N} \times \frac{e_2'}{2e_1' + e_2'},$$

(4.24)

where the last factor in the second equation accounts for the equilibrium energy distribution between the coupled symmetric stretch (ν_1) and bending (ν_2) vibrations. Here, e_1' and e_2' are the equilibrium average quantum numbers given by:

$$e_1' = \frac{1}{\exp\left(\frac{1920}{T_2}\right) - 1}, \quad e_2' = \frac{2}{\exp\left(\frac{960}{T_2}\right) - 1},$$

and T_2 is the vibrational temperature before the propagation of the pulse.

New vibrational temperatures are then calculated with Eq. 4.3.

Appendices

Appendix A

Cross-sections of excitation processes

Effective cross-sections are expressed in Å; their numerical values in the nodes are given in the tables below (linear interpolation must be used for determining the values in intermediate points); the data and citations are reproduced from [7].

The following notation for cross-sections is used:

Q_{m1} - Transport cross-section of CO_2 [17];

Q_{m2} - Transport cross-section of N_2 [11];

Q_{m3} - Transport cross-section of He [17];

Q - Cross-section of resonant excitation of N_2 rotation [18, 19];

Q_{11} - Cross-section of the process $(000) \rightarrow (01^10)$ [17];

Q_{12} - Cross-section of the process $(000) \rightarrow (100 + 020)$ [17];

$Q_{13}...Q_{16}$ - Cross-sections of resonant processes around 3.8 eV [17];

Q_{17} - Cross-section of the process $(000) \rightarrow (001)$ [17];

$Q_{18}...Q_{1,10}$ - Cross-sections of electronic excitation and ionization of CO_2 [10];

$Q_{21}...Q_{28}$ - Cross-sections of the process $N_2(v = 0) \rightarrow N_2(v = 1...8)$ [20, 21, 22];

$Q_{29}...Q_{2,15}$ - Cross-sections of electronic excitation and ionization of N_2 [22].

Table A.1: Cross-sections and energies for discharge pumping

u_i	Q_{m1}	u_i	Q_{m2}	u_i	Q_{m3}	u_i	Q
0	140	0	1.4	0	5	0.0015	0
0.04	84	0.001	1.4	0.01	5.4	0.05	0.1
0.1	55	0.002	1.6	0.1	5.8	0.25	0.65
0.3	21	0.008	2	0.2	6.2	0.5	1.15
0.5	10.8	0.01	2.2	1	6.5	0.8	2
0.6	9.4	0.04	4	2	6.1	1	2.65
1	5.7	0.08	6	7	5	1.5	5.6
1.7	5	0.1	6.5	10	4.1	1.8	7.5
2	5.1	0.2	8.8	20	3	1.9	8.2
2.5	6	0.3	9.8			2	8.6
3	7.7	0.4	10			2.15	8.95
4.1	9.4	1	10			2.43	9
5	14.5	1.2	11			2.6	8.9
7.4	10	1.4	12.5			2.75	8.4
10	11.7	1.8	20			2.9	7.65
20	16	2	25			3.25	6.2
27	16.3	2.5	30			3.6	5.1
50	13	3	26			4	4.5
		4	15			4.5	4.16
		5	12			5	3.97
		7	10			5.5	3.93
		10	10			7	4.17
		14	11			9	4.46
		18	12.2			11	4.42
		20	12			15	3.94
		30	10			22	3.15
		100	10			25	3.05

Table A.2: Cross-sections and energies for discharge pumping - continued

u_i	Q_{11}	u_i	Q_{12}	u_i	Q_{13}	u_i	Q_{14}	u_i	Q_{15}
0.083	0	0.167	0	0.252	0	2.37	0	2.37	0
0.085	0.36	0.2	0.54	2.7	0.25	3	0.26	3	0.17
0.09	1.04	0.25	0.82	3	0.4	3.5	0.52	3.65	0.33
0.1	1.6	0.3	0.82	3.3	0.6	4	0.5	3.8	0.31
0.12	1.84	0.5	0.68	3.6	0.65	4.5	0.22	4	0.21
0.14	2.12	0.7	0.56	4.5	0.23	4.6	0.1	4.3	0.1
0.16	2.16	1	0.47	4.6	0.1	5	0	5	0
0.2	2.08	1.4	0.45	5	0				
0.3	1.76	2	0.55						
0.4	1.52	3	1.15						
0.5	1.28	3.9	1.83						
0.6	1.08	4.5	1.4						
0.8	0.8	5	0.4						
1	0.58	6	0.28						
1.2	0.48	10	0.2						
1.6	0.34	20	0.1						
1.8	0.35								
2	0.4								
2.5	0.64								
3	1.04								
3.7	1.4								
4	1.36								
4.2	1.2								
4.5	0.92								
5	0.53								
6	0.4								
8	0.36								
9	0.28								
10	0.16								
10.1	0								
$u_{11} = 0.083$ eV		$u_{12} = 0.167$ eV		$u_{13} = 0.252$ eV		$u_{14} = 0.339$ eV		$u_{15} = 0.422$ eV	

u_i	Q_{16}	u_i	Q_{17}	u_i	Q_{18}	u_i	Q_{19}	u_i	$Q_{1,10}$
2.5	0	0.29	0	7	0	10.5	0	13.8	0
3	0.19	0.3	0.44	8	0.5	11.5	0.56	15	0.1
3.6	0.245	0.35	0.65	8.4	0.6	14	0.8	16	0.13
4	0.21	0.4	0.73	9	0.46	20	1.2	17	0.17
5.07	0	0.5	0.84	10	0.175	30	2	30	1.55
		0.8	1	10.5	0	50	4	40	2.1
		1	1						
		2	0.78						
		6	0.37						
		10	0.25						
		50	0						
$u_{16} = 2.5$ eV		$u_{17} = 0.29$ eV		$u_{18} = 7$ eV		$u_{19} = 10.5$ eV		$u_{1,10} = 13.8$ eV	

Table A.3: Cross-sections and energies for discharge pumping - continued

u_i	Q_{21}	u_i	Q_{22}	u_i	Q_{23}	u_i	Q_{24}	u_i	Q_{25}
0.29	0	1.83	0	1.9	0	2.05	0	2.1	0
0.5	0.0052	1.9	0.208	2	0.416	2.1	0.416	2.15	0.208
0.8	0.0083	2	1.46	2.1	1.33	2.2	1.16	2.2	0.541
1	0.0104	2.05	2.29	2.2	1.87	2.26	1.58	2.3	0.915
1.2	0.0166	2.1	1.66	2.3	1.25	2.55	0	2.46	1.12
1.3	0.0728	2.2	0.79	2.36	0.208	2.75	0.832	2.5	1.12
1.4	0.135	2.35	0.208	2.42	0	2.77	0	2.6	0.208
1.6	0.25	2.45	1.98	2.5	0.499	3	0.208	2.62	0
1.8	0.52	2.5	1.78	2.61	0.915	3.05	0.208	2.68	0
1.9	0.832	2.62	0.208	2.7	0.624	3.25	0	2.8	0.416
2	3.02	2.75	1.04	2.75	0.208			2.9	0.75
2.05	3.12	2.95	1.66	2.8	0			3	0
2.1	2.08	3.05	0.624	2.92	0.416			3.2	0.25
2.15	1.25	3.2	0.208	3	0.208			3.3	0.125
2.2	0.832	3.4	0.208	3.25	0.208			3.35	0
2.3	2.9	4	0	3.31	0				
2.45	1.04								
2.53	1.25								
2.6	1.75								
2.62	2.08								
2.68	1.73								
2.73	0.416								
2.85	0.32								
2.92	0.416								
3.12	0.728								
3.3	0.52								
4	0								
$u_{21} = 0.29$ eV		$u_{22} = 0.58$ eV		$u_{23} = 0.87$ eV		$u_{24} = 1.16$ eV		$u_{25} = 1.45$ eV	

u_i	Q_{26}	u_i	Q_{27}	u_i	Q_{28}	u_i	Q_{29}	u_i	$Q_{2,10}$
2.3	0	2.4	0	2.6	0	5	0	6.8	0
2.4	0.75	2.5	0.208	2.7	0.208	5.9	0.41	7.1	0.57
2.5	1.04	2.75	0.75	2.9	0.29	6.1	0.41	8.1	0.57
2.55	1.12	3	0	3	0.208	7	0.07	8.6	0.25
2.6	1.04	3.2	0.166	3.1	0	9	0	9.5	0.12
2.65	0.624	3.3	0.146	3.2	0			20.7	0
2.7	0.416	3.4	0	3.3	1.04				
2.8	0.208			3.4	0				
2.9	0.125								
3	2.5								
3.1	0.166								
3.2	0								
$u_{26} = 1.74$ eV		$u_{27} = 2.03$ eV		$u_{28} = 2.32$ eV		$u_{29} = 5$ eV		$u_{2,10} = 6.8$ eV	

u_i	$Q_{2,11}$	u_i	$Q_{2,12}$	u_i	$Q_{2,13}$	u_i	$Q_{2,14}$	u_i	$Q_{2,15}$
8.4	0	11.25	0	12.5	0	14	0	15.6	0
8.7	0.42	13.8	0.41	13	0.4	14.3	1.7	18	0.1
9.1	0.42	14	1	13.6	0.4	14.8	1.7	20	0.21
10	0.3	14.7	1	14	0.16	15.6	0.2	50	2.52
20.7	0	15	0.25	20.7	0	20.6	0.2	100	2.52
		65	0			25.4	2.8		
						100	2.8		
$u_{2,11} = 8.4$ eV		$u_{2,12} = 11.25$ eV		$u_{2,13} = 12.5$ eV		$u_{2,14} = 14$ eV		$u_{2,15} = 15.6$ eV	

Appendix B

Molecular constants

Use of data included in the HITRAN database and estimating missing rotational lines

In most cases, the transition frequencies and Einstein coefficients (A) for every rotational line of supported ro-vibrational bands are extracted directly from a HITRAN database `.par` file. The molecular constants (B) for each vibrational level can be obtained by fitting the transition frequencies listed in HITRAN with an analytical formula, as described later in this Appendix. However, the current version of HITRAN (HITRAN2020 [4]) lacks information on certain transitions that could potentially make a significant contribution to the amplification process. To address these gaps, we have supplemented the most critical missing data with rough estimates to enable more realistic modeling, albeit with limited precision.

Table B.1 lists the number of rotational lines in the P- and R-branches of each ro-vibrational band included in the **co2amp** model. The numbering of the ro-vibrational bands is consistent with Table 4.2. Table B.2 provides the Einstein coefficients (A) averaged over all P- and R-branch rotational lines included in HITRAN for a given ro-vibrational band. Note that the model uses the actual A values for each line; the averaged values are presented here for reference only. Additionally, the model includes only those lines where the rotational quantum numbers J for both the upper and lower levels do not exceed 59.

The model considers only P- and R-branch transitions. Although HITRAN includes Q-branch transitions for some bands in certain cases, their contribution to amplification is negligible due to their intensities being at least two orders of magnitude lower than those of the P- and R-branches.

Zeros in Table B.1 indicate that no rotational lines for a given ro-vibrational bands are present in HITRAN. Additionally, for some critical transitions, the number of included lines is very low (e.g., the first regular band for the 838 isotopologue has only 10 listed P- and R-branch lines combined). To address these critical gaps, we use the following approach:

1. Calculate the frequencies of missing transitions using the molecular constants obtained via the fitting procedure described later in this Appendix.

2. When adding additional lines to a band that already has some listed in HITRAN, assign the average Einstein coefficient (A) of the existing lines to the added transitions.

3. If no rotational lines for a given band are listed in HITRAN, roughly estimate the likely A coefficient by interpolating data from other isotopologues and ro-vibrational bands.

In cases where estimated lines are included in the **co2amp** distribution as separate `.par` files, an asterisk is placed in the corresponding field of Table B.1, and the estimated A coefficient is shown in Table B.2 in square brackets. Users can remove these additional `.par` files from the `hitran_data` folder to exclude them from calculations or add new `.par` files at their discretion. Care should be taken to avoid duplication of rotational lines across multiple `.par` files.

Table B.1: Numbers of P- and R-branch rotational lines in HITRAN2020 database

Band #	626	727	828	636	737	838	627	628	728	637	638	738
Regular bands												
0	99	24	57	87	0*	10*	152	165	93	119	135	0*
1	103	68	65	87	0*	28*	159	175	110	119	139	0*
Hot bands												
2e	89	0	30*	75	0	0	124	140	0	75	101	0
2f	89	0	29*	76	0	0	123	139	0	75	101	0
3e	92	0	44	77	0	0	133	149	44	79	107	0
3f	92	0	44	76	0	0	133	149	44	79	107	0
Sequence bands												
4	66	0	0*	44	0	0	0	13*	0	0	0	0
5	68	0	0*	41	0	0	0	60*	0	0	0	0
4-µm bands												
6	113	129	83	103	68	65	189	201	142	159	173	109
7	115	134	85	103	78	67	191	203	147	163	177	115
8e	111	127	81	101	72	48	185	197	138	157	171	109
8f	112	126	82	101	73	48	185	198	149	157	171	109

Table B.2: Einstein coefficients A of laser transitions, s^{-1} (averaged over all P and R lines).

Band #	626	727	828	636	737	838	627	628	728	637	638	738
Regular bands												
0	0.173	0.146	0.105	0.195	[0.18]	0.151	0.160	0.137	0.125	0.188	0.169	[0.16]
1	0.232	0.292	0.353	0.115	[0.17]	0.215	0.263	0.298	0.327	0.137	0.165	[0.19]
Hot bands												
2e	0.162	-	0.119	0.167	-	-	0.154	0.140	-	0.162	0.150	-
2f	0.161	-	0.118	0.166	-	-	0.154	0.139	-	0.162	0.150	-
3e	0.223	-	0.315	0.127	-	-	0.245	0.271	0.294	0.144	0.164	-
3f	0.225	-	0.317	0.128	-	-	0.246	0.272	0.295	0.144	0.164	-
Sequence bands												
4	0.391	-	[0.2]	0.422	-	-	-	0.310	-	-	-	-
5	0.420	-	[0.7]	0.200	-	-	-	0.543	-	-	-	-
4-µm bands												
6	196	195	188	176	173	167	196	193	192	175	172	171
7	197	195	186	178	174	168	196	192	191	177	174	172
8e	196	191	186	176	170	162	194	191	189	174	171	167
8f	197	191	186	176	170	163	194	191	189	174	171	167

Fitting procedure

Molecular constants of vibrational levels that can be used to calculate transition frequencies of ro-vibrational lines, including those not listed in the HITRAN database, can be often obtained by fitting the frequencies of the listed transitions. We have developed a fitting procedure that enabled finding molecular constants for nearly all vibratrional levels of all CO_2 isotopologues included in the `co2amp` model. The fitting procedure is described in the hollowing section following by the list of the molecular constants obtained using this procedure for all the isotopolagues.

The fitting procedure is performed using the `hitran_ExtractAndFit.py` script. The fitting formula is as follows:

$$F(v, J) = G_v + B_v J(J+1) - D_v[J(J+1)]^2 + H_v[J(J+1)]^3 + L_v[J(J+1)]^4 \qquad \text{(B.1)}$$

Table B.3: Fitting procedure using HITRAN data.

Step	Obtain molecular constants for levels:	using HITRAN frequencies of these transitions:	with these fitting parameters fixed:
1	00^00 10^01	$00^01 \to 00^00(e)$	$G(\text{lower level}) = 0$
2	$10^01(1)$ $10^01(2)$	$10^01(1) \to 00^00(e)$ $10^01(2) \to 00^00(e)$	All lower-level parameters
3	$01^{1e}0$ & $G(01^{1f}0) = G(01^{1e}0)$	$01^10 \to 00^00(e)$	All lower-level parameters
4	$02^{2e}0$ & $G(02^{2f}0) = G(02^{2e}0)$	$02^20 \to 01^10(e)$	All lower-level parameters
5	$01^{1e}1$	$01^11 \to 01^10(e)$	All lower-level parameters
6	$01^{1f}0$ $02^{2f}0$	$02^20 \to 01^10(f)$	$G(\text{upper level})$ $G(\text{lower level})$
7	$01^{1f}1$	$01^11 \to 01^10(f)$	All lower-level parameters
8	$02^{2f}1$ $03^{3f}0$ $11^{1f}0(1)$ $11^{1f}0(2)$	$02^21 \to 02^20(f)$ $03^30 \to 02^20(f)$ $11^10(1) \to 02^20(f)$ $11^10(2) \to 02^20(f)$	All lower-level parameters
9	$02^{2e}1$ $03^{3e}0$ $11^{1e}0(1)$ $11^{1e}0(2)$	$02^21 \to 02^20(e)$ $03^30 \to 02^20(e)$ $11^10(1) \to 02^20(e)$ $11^10(2) \to 02^20(e)$	All lower-level parameters
10	00^02	$00^02 \to 00^01(e)$	All lower-level parameters
11	$10^00(1)$ $10^00(2)$	$10^01(1) \to 10^00(1)(e)$ $10^01(2) \to 10^00(2)(e)$	All upper-level parameters

Lists of molecular constants

Tables B.4 through B.15 present the molecular constants for the twelve isotopologues of CO_2 supported by the `co2amp` model. These constants were derived by fitting HITRAN2020 data using the procedure described earlier in this Appendix.

Table B.4: Molecular constants for the *626* isotopologue of CO_2 (co2amp #: '0'; HITRAN ID: '1').

#	Level	G (Hz)	B (Hz)	D (Hz)	H (Hz)	L (Hz)
			Ground state			
	00^00	0.000000e+00	1.169847e+10	3.997874e+03	3.422140e-04	1.833945e-09
			0 1 0			
	$01^{1e}0$	2.000755e+13	1.171107e+10	4.056805e+03	4.613985e-04	1.687720e-09
	$01^{1f}0$	2.000755e+13	1.172952e+10	4.079350e+03	4.030478e-04	4.238366e-09
			0 0 1			
0	0^001	7.042553e+13	1.160620e+10	3.987269e+03	3.645313e-04	2.353858e-09
			1 0 0 + 0 2 0			
1	$[10^00, 02^00]_I$	4.161676e+13	1.169758e+10	3.452278e+03	6.858418e-03	-6.367059e-08
2	$[10^00, 02^00]_{II}$	1.083102e+14	1.161705e+10	4.722355e+03	6.514604e-03	-1.655007e-08
3	$02^{2e}0$	4.002624e+13	1.174187e+10	4.114234e+03	-1.219793e-02	9.123448e-08
4	$02^{2f}0$	4.002624e+13	1.174187e+10	4.137902e+03	5.025296e-04	4.783869e-09
			0 1 1			
5	$01^{1e}1$	9.005802e+13	1.161974e+10	4.041027e+03	5.619003e-04	3.543866e-09
6	$01^{1f}1$	9.005802e+13	1.163765e+10	4.069479e+03	4.446209e-04	5.071835e-09
			1 1 0 + 0 3 0			
7	$[11^{1e}0, 03^{1e}0]_I$	6.226257e+13	1.170419e+10	3.769087e+03	1.800030e-03	8.158086e-08
8	$[11^{1e}0, 03^{1e}0]_{II}$	5.793400e+13	1.171424e+10	4.477417e+03	2.843734e-03	5.894220e-09
9	$[11^{1f}0, 03^{1f}0]_I$	6.226257e+13	1.173189e+10	3.632993e+03	2.079957e-03	-4.705525e-08
10	$[11^{1f}0, 03^{1f}0]_{II}$	5.793400e+13	1.174257e+10	4.685703e+03	3.061140e-03	2.754524e-08
11	$03^{3e}0$	6.005580e+13	1.176322e+10	4.200887e+03	-4.188810e-03	-2.044073e-08
12	$03^{3f}0$	6.005581e+13	1.176321e+10	4.199437e+03	-3.650476e-03	3.794673e-08
			0 0 2			
13	0^002	1.401028e+14	1.151401e+10	3.977393e+03	3.520213e-04	4.404983e-09
			1 0 1 + 0 2 1			
14	$[10^01, 02^01]_I$	1.113664e+14	1.160387e+10	3.431869e+03	6.923863e-03	-6.121059e-08
15	$[10^01, 02^01]_{II}$	1.083102e+14	1.161705e+10	4.722355e+03	6.514604e-03	-1.655007e-08
16	$02^{2e}1$	1.097022e+14	1.165102e+10	4.072805e+03	-1.153052e-02	9.005439e-08
17	$02^{2f}1$	1.097022e+14	1.165102e+10	4.120733e+03	6.447142e-04	9.308838e-09

Table B.5: Molecular constants for the 727 isotopologue of CO_2 (co2amp #: '1'; HITRAN ID: '9').

#	Level	G (Hz)	B (Hz)	D (Hz)	H (Hz)	L (Hz)
				Ground state		
	00^00	0.000000e+00	1.100821e+10	3.540269e+03	3.045913e-04	2.200121e-09
				0 1 0		
	$01^{1e}0$	1.984824e+13	1.102072e+10	3.592409e+03	3.534507e-04	6.968897e-09
	$01^{1f}0$	1.984824e+13	1.103721e+10	3.627170e+03	5.884566e-03	-6.150162e-07
				0 0 1		
0	0^001	6.986942e+13	1.092154e+10	3.531384e+03	3.248925e-04	2.290272e-09
				1 0 0 + 0 2 0		
1	$[10^00, 02^00]_I$	4.091988e+13	1.101834e+10	3.050116e+03	3.440943e-03	-2.829718e-08
2	$[10^00, 02^00]_{II}$	3.772097e+13	1.100609e+10	4.068545e+03	5.636968e-03	2.606318e-08
3	$02^{2e}0$	3.970844e+13	1.104948e+10	3.748356e+03	-8.317792e-03	4.797954e-08
4	$02^{2f}0$	3.970844e+13	1.104948e+10	3.666397e+03	1.880498e-03	-1.824074e-07
				0 1 1		
5	$01^{1e}1$	8.934676e+13	1.093484e+10	3.579202e+03	2.866502e-04	1.957388e-08
6	$01^{1f}1$	8.934676e+13	1.095089e+10	3.615057e+03	4.650449e-03	-4.939190e-07
				1 1 0 + 0 3 0		
7	$[11^{1e}0, 03^{1e}0]_I$	6.140119e+13	1.102176e+10	3.331424e+03	-5.173688e-03	2.091981e-06
8	$[11^{1e}0, 03^{1e}0]_{II}$	5.696820e+13	1.101815e+10	3.931319e+03	3.100101e-03	-1.395438e-08
9	$[11^{1f}0, 03^{1f}0]_I$	6.140119e+13	1.104810e+10	3.230829e+03	1.803753e-03	-1.022061e-07
10	$[11^{1f}0, 03^{1f}0]_{II}$	5.696820e+13	1.104180e+10	4.104803e+03	1.163940e-02	-2.660330e-06
11	$03^{3e}0$	5.958039e+13	1.106979e+10	3.758888e+03	-2.332341e-03	-1.689152e-07
12	$03^{3f}0$	5.958039e+13	1.106979e+10	3.760631e+03	-6.395446e-04	-2.032602e-07
				0 0 2		
13	0^002	1.389995e+14	1.083494e+10	3.536112e+03	1.197349e-02	-3.265901e-06
				1 0 1 + 0 2 1		
14	$[10^01, 02^01]_I$	1.101047e+14	1.093044e+10	3.019817e+03	2.825733e-03	1.634035e-08
15	$[10^01, 02^01]_{II}$	1.069801e+14	1.092190e+10	4.097907e+03	5.878832e-03	1.522123e-08
16	$02^{2e}1$	1.088366e+14	1.096402e+10	3.709288e+03	-8.065366e-03	7.193800e-08
17	$02^{2f}1$	1.088366e+14	1.096402e+10	3.650702e+03	1.054827e-03	-6.412082e-08

Table B.6: Molecular constants for the *828* isotopologue of CO_2 (co2amp #: '2'; HITRAN ID: '7').

#	Level	G (Hz)	B (Hz)	D (Hz)	H (Hz)	L (Hz)
				Ground state		
	00^00	0.000000e+00	1.039731e+10	3.159169e+03	4.731420e-04	-8.574308e-09
				0 1 0		
	$01^{1e}0$	1.970621e+13	1.040967e+10	3.208038e+03	5.553249e-04	-8.713116e-09
	$01^{1f}0$	1.970621e+13	1.042447e+10	3.217114e+03	-5.350701e-04	6.086616e-08
				0 0 1		
0	0^001	6.937342e+13	1.031556e+10	3.151903e+03	4.829303e-04	-8.466869e-09
				1 0 0 + 0 2 0		
1	$[10^00, 02^00]_I$	4.038480e+13	1.041490e+10	2.770578e+03	3.122068e-03	-6.107233e-08
2	$[10^00, 02^00]_{II}$	3.688419e+13	1.038853e+10	3.519518e+03	4.940659e-03	-4.420393e-08
3	$02^{2e}0$	3.942513e+13	1.043663e+10	3.411526e+03	-6.330581e-03	7.740561e-08
4	$02^{2f}0$	3.942513e+13	1.043663e+10	3.267584e+03	-9.697851e-05	3.691415e-08
				0 1 1		
5	$01^{1e}1$	8.871241e+13	1.032862e+10	3.198300e+03	6.116848e-04	-7.437619e-09
6	$01^{1f}1$	8.871241e+13	1.034305e+10	3.211021e+03	-4.142739e-04	5.457863e-08
				1 1 0 + 0 3 0		
7	$[11^{1e}0, 03^{1e}0]_I$	6.069384e+13	1.041665e+10	2.996559e+03	1.464180e-03	5.957494e-08
8	$[11^{1e}0, 03^{1e}0]_{II}$	5.602234e+13	1.040290e+10	3.470006e+03	2.545506e-03	-2.768221e-08
9	$[11^{1f}0, 03^{1f}0]_I$	6.069384e+13	1.044155e+10	2.915684e+03	-8.769903e-04	1.246696e-08
10	$[11^{1f}0, 03^{1f}0]_{II}$	5.602234e+13	1.042292e+10	3.587647e+03	3.198738e-03	-4.725434e-08
11	$03^{3e}0$	5.915649e+13	1.045597e+10	3.380122e+03	-2.659957e-03	-6.784026e-09
12	$03^{3f}0$	5.915649e+13	1.045598e+10	3.377600e+03	-1.972042e-03	6.128165e-08
				0 0 2		
13	0^002	1.380154e+14	1.023388e+10	3.142644e+03	-4.160245e-04	9.296848e-08
				1 0 1 + 0 2 1		
14	$[10^01, 02^01]_I$	1.090664e+14	1.033240e+10	2.746883e+03	2.603971e-03	-4.874926e-08
15	$[10^01, 02^01]_{II}$	1.056829e+14	1.030862e+10	3.547531e+03	5.301334e-03	-4.288713e-08
16	$02^{2e}1$	1.080647e+14	1.035596e+10	3.377649e+03	-5.964667e-03	6.909073e-08
17	$02^{2f}1$	1.080647e+14	1.035596e+10	3.257854e+03	1.036638e-04	3.029389e-08

Table B.7: Molecular constants for the *636* isotopologue of CO_2 (co2amp #: '3'; HITRAN ID: '2').

#	Level	G (Hz)	B (Hz)	D (Hz)	H (Hz)	L (Hz)
				Ground state		
	00^00	0.000000e+00	1.169902e+10	3.996787e+03	4.870281e-04	-2.688092e-09
				0 1 0		
	$01^{1e}0$	1.944089e+13	1.171021e+10	4.053157e+03	5.984974e-04	-2.608336e-09
	$01^{1f}0$	1.944089e+13	1.172919e+10	4.071961e+03	7.921901e-05	1.905386e-08
				0 0 1		
0	$0^00 1$	6.845722e+13	1.161017e+10	3.985398e+03	5.208250e-04	-2.085314e-09
				1 0 0 + 0 2 0		
1	$[10^00, 02^00]_I$	4.107342e+13	1.168345e+10	3.606041e+03	6.533067e-03	6.119090e-08
2	$[10^00, 02^00]_{II}$	3.794852e+13	1.171937e+10	4.749446e+03	8.650202e-03	-1.005383e-07
3	$02^{2e}0$	3.889102e+13	1.174016e+10	3.907318e+03	-1.328696e-02	2.913526e-08
4	$02^{2f}0$	3.889102e+13	1.174015e+10	4.128991e+03	3.050528e-04	1.409386e-08
				0 1 1		
5	$01^{1e}1$	8.754654e+13	1.162234e+10	4.034971e+03	7.067286e-04	5.524693e-10
6	$01^{1f}1$	8.754654e+13	1.164072e+10	4.061159e+03	1.502934e-04	1.930438e-08
				1 1 0 + 0 3 0		
7	$[11^{1e}0, 03^{1e}0]_I$	6.107053e+13	1.171940e+10	3.695536e+03	3.427727e-03	3.216981e-10
8	$[11^{1e}0, 03^{1e}0]_{II}$	5.685676e+13	1.175251e+10	4.683189e+03	1.249661e-03	5.682444e-08
9	$[11^{1f}0, 03^{1f}0]_I$	6.107053e+13	1.169343e+10	3.824401e+03	2.561340e-03	4.579441e-08
10	$[11^{1f}0, 03^{1f}0]_{II}$	5.685676e+13	1.172081e+10	4.494696e+03	4.454015e-03	-5.659966e-08
11	$03^{3e}0$	5.835015e+13	1.176039e+10	4.114817e+03	-5.167970e-03	2.030431e-08
12	$03^{3f}0$	5.835015e+13	1.176037e+10	4.109583e+03	-3.908309e-03	-1.314619e-09
				0 0 2		
13	$0^00 2$	1.362121e+14	1.152137e+10	3.975073e+03	5.727161e-04	-3.125152e-09
				1 0 1 + 0 2 1		
14	$[10^01, 02^01]_I$	1.089119e+14	1.159370e+10	3.598631e+03	6.594981e-03	6.086349e-08
15	$[10^01, 02^01]_{II}$	1.057589e+14	1.163304e+10	4.733620e+03	8.757636e-03	-1.066724e-07
16	$02^{2e}1$	1.066456e+14	1.165276e+10	3.872393e+03	-1.296110e-02	4.841050e-08
17	$02^{2f}1$	1.066456e+14	1.165275e+10	4.108754e+03	4.999532e-04	1.939811e-08

Table B.8: Molecular constants for the *737* isotopologue of CO_2 (co2amp #: '4'; HITRAN ID: 'B').

#	Level	G (Hz)	B (Hz)	D (Hz)	H (Hz)	L (Hz)
Ground state						
	00^00	0.000000e+00	1.100873e+10	3.526660e+03	-3.776171e-03	7.450271e-07
0 1 0						
	$01^{1e}0$	1.927670e+13	1.101991e+10	3.574795e+03	-3.546434e-03	7.182690e-07
	$01^{1f}0$	1.927670e+13	1.103691e+10	3.665475e+03	6.416756e-02	-2.107236e-05
0 0 1						
0	0^001	6.788379e+13	1.092526e+10	3.517266e+03	-3.940367e-03	7.836869e-07
1 0 0 + 0 2 0						
1	$[10^00, 02^00]_I$	4.020974e+13	1.100435e+10	3.055858e+03	-1.278980e-02	5.779730e-06
2	$[10^00, 02^00]_{II}$	3.729090e+13	1.101899e+10	4.153649e+03	-4.931876e-03	2.465591e-06
3	$02^{2e}0$	3.856347e+13	1.104786e+10	3.591065e+03	-1.405369e-02	9.337185e-07
4	$02^{2f}0$	3.856347e+13	1.104785e+10	3.647374e+03	7.979279e-03	-4.985772e-06
0 1 1						
5	$01^{1e}1$	8.681306e+13	1.093728e+10	3.564038e+03	-1.798705e-03	3.896102e-07
6	$01^{1f}1$	8.681307e+13	1.095377e+10	3.610054e+03	2.793970e-02	-1.262047e-05
1 1 0 + 0 3 0						
7	—	-	-	-	-	-
8	—	-	-	-	-	-
0 0 2						
13	—	-	-	-	-	-
1 0 1 + 0 2 1						
14	$[10^01, 02^01]_I$	1.074725e+14	1.091963e+10	3.056680e+03	1.270003e-03	7.400413e-07
15	$[10^01, 02^01]_{II}$	1.045617e+14	1.093815e+10	4.160861e+03	-1.042790e-03	1.220240e-06
16	$02^{2e}1$	1.057530e+14	1.096565e+10	3.563570e+03	-7.599727e-03	-8.775706e-07
17	$02^{2f}1$	1.057530e+14	1.096564e+10	3.626319e+03	7.721920e-05	-2.054072e-06

Table B.9: Molecular constants for the *838* isotopologue of CO_2 (co2amp #: '5'; HITRAN ID: '0').

#	Level	G (Hz)	B (Hz)	D (Hz)	H (Hz)	L (Hz)
				Ground state		
	00^00	0.000000e+00	1.039780e+10	3.154063e+03	1.402651e-05	1.428556e-08
				0 1 0		
	$01^{1e}0$	1.913019e+13	1.040897e+10	3.198383e+03	9.342027e-06	2.176834e-08
	$01^{1f}0$	1.913019e+13	1.042416e+10	3.213009e+03	-1.120423e-03	1.665888e-07
				0 0 1		
0	0^001	6.737208e+13	1.031909e+10	3.146124e+03	-4.247794e-05	1.873665e-08
				1 0 0 + 0 2 0		
1	$[10^00, 02^00]_I$	3.953352e+13	1.040346e+10	2.716362e+03	2.823526e-03	2.282443e-08
2	$[10^00, 02^00]_{II}$	3.658622e+13	1.039897e+10	3.655001e+03	4.770731e-03	6.161621e-09
3	$02^{2e}0$	3.827120e+13	1.043513e+10	3.303245e+03	-7.568352e-03	5.104746e-08
4	$02^{2f}0$	3.827120e+13	1.043513e+10	3.260995e+03	1.063659e-04	4.317807e-08
				0 1 1		
5	$01^{1e}1$	8.615853e+13	1.033097e+10	3.187081e+03	-1.626456e-04	4.082526e-08
6	$01^{1f}1$	8.615853e+13	1.034577e+10	3.208362e+03	-4.474011e-04	1.082095e-07
				1 1 0 + 0 3 0		
7	$[11^{1e}0, 03^{1e}0]_I$	5.926637e+13	1.040754e+10	2.988158e+03	1.539636e-02	-4.566861e-06
8	$[11^{1e}0, 03^{1e}0]_{II}$	5.514265e+13	1.040849e+10	3.506383e+03	1.763155e-03	3.816660e-07
9	$[11^{1f}0, 03^{1f}0]_I$	5.926637e+13	1.043130e+10	2.866227e+03	-5.732561e-03	2.293647e-06
10	$[11^{1f}0, 03^{1f}0]_{II}$	5.514265e+13	1.043085e+10	3.662187e+03	5.008245e-03	-9.262836e-07
11	$03^{3e}0$	5.742282e+13	1.045349e+10	3.326196e+03	-5.079115e-03	4.246875e-07
12	$03^{3f}0$	5.742282e+13	1.045349e+10	3.328606e+03	-3.564036e-03	3.126050e-07
				0 0 2		
13	0^002	1.340587e+14	1.024044e+10	3.135498e+03	-3.190897e-03	9.014456e-07
				1 0 1 + 0 2 1		
14	$[10^01, 02^01]_I$	1.062772e+14	1.032355e+10	2.696401e+03	2.969989e-03	-4.648862e-09
15	$[10^01, 02^01]_{II}$	1.033808e+14	1.032260e+10	3.675030e+03	4.691872e-03	1.168720e-08
16	$02^{2e}1$	1.049562e+14	1.035750e+10	3.270427e+03	-7.862088e-03	1.806708e-07
17	$02^{2f}1$	1.049562e+14	1.035750e+10	3.246181e+03	-2.511702e-03	6.130943e-07

Table B.10: Molecular constants for the *627* isotopologue of CO_2 (co2amp #: '6'; HITRAN ID: '4').

#	Level	G (Hz)	B (Hz)	D (Hz)	H (Hz)	L (Hz)
				Ground state		
	00^00	0.000000e+00	1.135055e+10	3.764163e+03	3.773335e-04	-2.267907e-10
				0 1 0		
	$01^{1e}0$	1.992806e+13	1.136310e+10	3.819162e+03	4.927354e-04	-7.306791e-10
	$01^{1f}0$	1.992806e+13	1.138055e+10	3.840989e+03	4.181522e-04	4.480501e-09
				0 0 1		
0	0^001	7.015184e+13	1.126112e+10	3.754512e+03	3.800540e-04	7.603355e-10
				1 0 0 + 0 2 0		
1	$[10^00, 02^00]_I$	4.125222e+13	1.135549e+10	3.232958e+03	4.720317e-03	-3.837020e-08
2	$[10^00, 02^00]_{II}$	3.814223e+13	1.135312e+10	4.389746e+03	6.724376e-03	-3.068154e-08
3	$02^{2e}0$	3.986768e+13	1.139287e+10	3.934794e+03	-9.909214e-03	6.663958e-08
4	$02^{2f}0$	3.986768e+13	1.139288e+10	3.897079e+03	7.344429e-04	-6.369967e-09
				0 1 1		
5	$01^{1e}1$	8.970696e+13	1.127453e+10	3.805655e+03	6.043847e-04	-8.459386e-10
6	$01^{1f}1$	8.970696e+13	1.129150e+10	3.832299e+03	4.570792e-04	4.722654e-09
				1 1 0 + 0 3 0		
7	$[11^{1e}0, 03^{1e}0]_I$	6.182016e+13	1.136035e+10	3.543847e+03	1.791605e-03	7.110069e-08
8	$[11^{1e}0, 03^{1e}0]_{II}$	5.746100e+13	1.136325e+10	4.200221e+03	2.729130e-03	1.251955e-08
9	$[11^{1f}0, 03^{1f}0]_I$	6.182016e+13	1.138743e+10	3.423918e+03	1.346351e-03	-5.173594e-08
10	$[11^{1f}0, 03^{1f}0]_{II}$	5.746100e+13	1.138916e+10	4.389403e+03	3.714234e-03	-3.819197e-09
11	$03^{3e}0$	5.981858e+13	1.141368e+10	3.976029e+03	-3.743588e-03	-9.046605e-09
12	$03^{3f}0$	3.986768e+13	1.139288e+10	3.897079e+03	7.344429e-04	-6.369967e-09
				0 0 2		
13	0^002	1.395595e+14	1.117175e+10	3.745298e+03	2.985246e-04	8.302926e-09
				1 0 1 + 0 2 1		
14	$[10^01, 02^01]_I$	1.107240e+14	1.126467e+10	3.207000e+03	4.689076e-03	-4.032129e-08
15	$[10^01, 02^01]_{II}$	1.076636e+14	1.126646e+10	4.412595e+03	6.541735e-03	-2.007530e-08
16	$02^{2e}1$	1.092742e+14	1.130474e+10	3.894968e+03	-9.392562e-03	6.599009e-08
17	$02^{2f}1$	1.092742e+14	1.130475e+10	3.882272e+03	8.200398e-04	-1.312426e-09

Table B.11: Molecular constants for the *628* isotopologue of CO_2 (co2amp #: '7'; HITRAN ID: '3').

#	Level	G (Hz)	B (Hz)	D (Hz)	H (Hz)	L (Hz)
				Ground state		
	00^00	0.000000e+00	1.103789e+10	3.560050e+03	3.143585e-04	9.557979e-10
				0 1 0		
	$01^{1e}0$	1.985746e+13	1.105040e+10	3.611888e+03	4.003987e-04	1.513565e-09
	$01^{1f}0$	1.985746e+13	1.106696e+10	3.634829e+03	9.810914e-04	-2.596685e-08
				0 0 1		
0	$0^00 1$	6.991497e+13	1.095102e+10	3.551154e+03	3.301286e-04	1.277276e-09
				1 0 0 + 0 2 0		
1	$[10^00, 02^00]_I$	4.094694e+13	1.104772e+10	3.068769e+03	4.181464e-03	-6.010828e-08
2	$[10^00, 02^00]_{II}$	3.775661e+13	1.103600e+10	4.097679e+03	6.254021e-03	-3.379214e-08
3	$02^{2e}0$	3.972688e+13	1.107923e+10	3.762843e+03	-9.097657e-03	9.381927e-08
4	$02^{2f}0$	3.972688e+13	1.107924e+10	3.683947e+03	7.201636e-04	-9.670807e-09
				0 1 1		
5	$01^{1e}1$	8.940144e+13	1.096433e+10	3.599364e+03	4.851830e-04	1.735324e-09
6	$01^{1f}1$	8.940144e+13	1.098045e+10	3.626504e+03	9.647165e-04	-2.332943e-08
				1 1 0 + 0 3 0		
7	$[11^{1e}0, 03^{1e}0]_I$	6.143764e+13	1.105119e+10	3.355164e+03	1.438697e-03	7.934392e-08
8	$[11^{1e}0, 03^{1e}0]_{II}$	5.701264e+13	1.104793e+10	3.951529e+03	2.304154e-03	1.895828e-08
9	$[11^{1f}0, 03^{1f}0]_I$	6.143764e+13	1.107763e+10	3.245377e+03	7.480496e-04	-4.772488e-08
10	$[11^{1f}0, 03^{1f}0]_{II}$	5.701264e+13	1.107176e+10	4.121874e+03	3.558591e-03	3.813976e-09
11	$03^{3e}0$	5.960795e+13	1.109957e+10	3.774488e+03	-3.377326e-03	-1.980484e-08
12	$03^{3f}0$	5.960795e+13	1.109958e+10	3.776461e+03	-2.225695e-03	2.389924e-08
				0 0 2		
13	$0^00 2$	1.390888e+14	1.086421e+10	3.542835e+03	3.316297e-04	2.579492e-09
				1 0 1 + 0 2 1		
14	$[10^01, 02^01]_I$	1.101777e+14	1.095961e+10	3.039141e+03	3.836002e-03	-5.429492e-08
15	$[10^01, 02^01]_{II}$	1.070601e+14	1.095164e+10	4.126369e+03	6.312306e-03	-2.519441e-08
16	$02^{2e}1$	1.089005e+14	1.099359e+10	3.724561e+03	-8.569755e-03	8.574433e-08
17	$02^{2f}1$	1.089005e+14	1.099360e+10	3.670639e+03	8.021495e-04	-6.665057e-09

Table B.12: Molecular constants for the *728* isotopologue of CO_2 (co2amp #: '8'; HITRAN ID: '8').

#	Level	G (Hz)	B (Hz)	D (Hz)	H (Hz)	L (Hz)
				Ground state		
	00^00	0.000000e+00	1.070053e+10	3.341861e+03	3.051059e-06	1.717260e-08
				0 1 0		
	$01^{1e}0$	1.977734e+13	1.071297e+10	3.391254e+03	8.829789e-05	1.750289e-08
	$01^{1f}0$	1.977734e+13	1.072860e+10	3.414083e+03	1.304750e-03	-7.837745e-08
				0 0 1		
0	0^001	6.962484e+13	1.061635e+10	3.333954e+03	-3.189537e-05	2.042003e-08
				1 0 0 + 0 2 0		
1	$[10^00, 02^00]_I$	4.064148e+13	1.071477e+10	2.900403e+03	2.662506e-03	-1.209968e-08
2	$[10^00, 02^00]_{II}$	3.731199e+13	1.069471e+10	3.783607e+03	5.256232e-03	-2.006028e-08
3	$02^{2e}0$	3.956702e+13	1.074082e+10	3.575078e+03	-7.624378e-03	8.632104e-08
4	$02^{2f}0$	3.956702e+13	1.074082e+10	3.458161e+03	1.629631e-04	1.887195e-08
				0 1 1		
5	$01^{1e}1$	8.903315e+13	1.062954e+10	3.380817e+03	2.479090e-04	8.621822e-09
6	$01^{1f}1$	8.903315e+13	1.064476e+10	3.406456e+03	1.127887e-03	-6.298039e-08
				1 1 0 + 0 3 0		
7	$[11^{1e}0, 03^{1e}0]_I$	6.103891e+13	1.071717e+10	3.152678e+03	-5.122530e-04	3.356267e-07
8	$[11^{1e}0, 03^{1e}0]_{II}$	5.650260e+13	1.070814e+10	3.688354e+03	6.767040e-04	2.755581e-07
9	$[11^{1f}0, 03^{1f}0]_I$	6.103890e+13	1.074282e+10	3.063909e+03	-8.519336e-04	7.049229e-08
10	$[11^{1f}0, 03^{1f}0]_{II}$	5.650260e+13	1.072988e+10	3.835517e+03	4.248794e-03	-1.883085e-07
11	$03^{3e}0$	5.936887e+13	1.076064e+10	3.561005e+03	-3.067349e-03	-1.281520e-08
12	$03^{3f}0$	5.936887e+13	1.076064e+10	3.560716e+03	-2.282685e-03	6.394468e-08
				0 0 2		
13	0^002	1.385140e+14	1.053223e+10	3.322526e+03	-2.172402e-03	3.512198e-07
				1 0 1 + 0 2 1		
14	$[10^01, 02^01]_I$	1.095778e+14	1.062959e+10	2.871511e+03	1.961680e-03	1.966607e-08
15	$[10^01, 02^01]_{II}$	1.063448e+14	1.061270e+10	3.813989e+03	5.427167e-03	-6.930661e-09
16	$02^{2e}1$	1.084544e+14	1.065778e+10	3.540689e+03	-6.829286e-03	4.079148e-08
17	$02^{2f}1$	1.084544e+14	1.065778e+10	3.446796e+03	1.626387e-04	2.879651e-08

Table B.13: Molecular constants for the *637* isotopologue of CO_2 (co2amp #: '9'; HITRAN ID: '6').

#	Level	G (Hz)	B (Hz)	D (Hz)	H (Hz)	L (Hz)
			Ground state			
	00^00	0.000000e+00	1.135090e+10	3.751993e+03	3.295724e-04	1.848790e-09
			0 1 0			
	$01^{1e}0$	1.935898e+13	1.136209e+10	3.800997e+03	4.291947e-04	2.279936e-09
	$01^{1f}0$	1.935898e+13	1.138006e+10	3.823285e+03	-1.422896e-03	1.410492e-07
			0 0 1			
0	0^001	6.817541e+13	1.126478e+10	3.741138e+03	3.569578e-04	2.398138e-09
			1 0 0 + 0 2 0			
1	$[10^00, 02^00]_I$	4.062495e+13	1.134084e+10	3.315706e+03	5.995566e-03	3.738754e-08
2	$[10^00, 02^00]_{II}$	3.763366e+13	1.136629e+10	4.447889e+03	6.800443e-03	-5.898947e-08
3	$02^{2e}0$	3.872764e+13	1.139104e+10	3.749358e+03	-1.150982e-02	3.312430e-08
4	$02^{2f}0$	3.872764e+13	1.139104e+10	3.876044e+03	-4.694316e-04	8.018623e-08
			0 1 1			
5	$01^{1e}1$	8.718494e+13	1.127687e+10	3.784144e+03	4.888290e-04	7.118700e-09
6	$01^{1f}1$	8.718494e+13	1.129431e+10	3.814201e+03	-1.115188e-03	1.231015e-07
			1 1 0 + 0 3 0			
7	$[11^{1e}0, 03^{1e}0]_I$	6.056383e+13	1.134948e+10	3.562716e+03	2.237169e-03	6.106637e-08
8	$[11^{1e}0, 03^{1e}0]_{II}$	5.643763e+13	1.136969e+10	4.206447e+03	3.610740e-03	-3.390843e-08
9	$[11^{1f}0, 03^{1f}0]_I$	6.056383e+13	1.137491e+10	3.437890e+03	1.728200e-03	8.184400e-08
10	$[11^{1f}0, 03^{1f}0]_{II}$	5.643763e+13	1.139879e+10	4.410018e+03	1.128607e-03	9.918617e-08
11	$03^{3e}0$	5.810565e+13	1.141078e+10	3.893156e+03	-4.778181e-03	4.420741e-08
12	$03^{3f}0$	5.810565e+13	1.141078e+10	3.889556e+03	-4.281835e-03	7.159137e-08
			0 0 2			
13	0^002	1.356526e+14	1.117871e+10	3.730558e+03	1.169536e-04	3.754630e-08
			1 0 1 + 0 2 1			
14	$[10^01, 02^01]_I$	1.081816e+14	1.125361e+10	3.307496e+03	6.136004e-03	3.642407e-08
15	$[10^01, 02^01]_{II}$	1.051784e+14	1.128278e+10	4.439767e+03	6.739638e-03	-6.389357e-08
16	$02^{2e}1$	1.062047e+14	1.130627e+10	3.712975e+03	-1.118484e-02	4.803879e-08
17	$02^{2f}1$	1.062047e+14	1.130627e+10	3.858128e+03	-2.815269e-04	8.076280e-08

Table B.14: Molecular constants for the *638* isotopologue of CO_2 (co2amp #: '10'; HITRAN ID: '5').

#	Level	G (Hz)	B (Hz)	D (Hz)	H (Hz)	L (Hz)
			Ground state			
	00^00	0.000000e+00	1.103782e+10	3.558680e+03	5.050129e-04	-6.840577e-09
			0 1 0			
	$01^{1e}0$	1.928621e+13	1.104901e+10	3.609360e+03	6.153830e-04	-7.852508e-09
	$01^{1f}0$	1.928621e+13	1.106606e+10	3.632513e+03	1.386175e-03	-6.096041e-08
			0 0 1			
0	0^001	6.793212e+13	1.095417e+10	3.549653e+03	5.217531e-04	-6.604860e-09
			1 0 0 + 0 2 0			
1	$[10^00, 02^00]_I$	4.024045e+13	1.103310e+10	3.099093e+03	5.432427e-03	6.773242e-09
2	$[10^00, 02^00]_{II}$	3.732115e+13	1.104839e+10	4.198794e+03	5.926794e-03	-3.889335e-08
3	$02^{2e}0$	3.858248e+13	1.107703e+10	3.620566e+03	-9.533108e-03	1.183483e-08
4	$02^{2f}0$	3.858248e+13	1.107703e+10	3.679687e+03	8.777259e-04	-2.403959e-08
			0 1 1			
5	$01^{1e}1$	8.687084e+13	1.096620e+10	3.596410e+03	6.854043e-04	-7.012776e-09
6	$01^{1f}1$	8.687084e+13	1.098276e+10	3.623708e+03	1.307980e-03	-5.402701e-08
			1 1 0 + 0 3 0			
7	$[11^{1e}0, 03^{1e}0]_I$	6.012168e+13	1.104022e+10	3.368027e+03	2.333566e-03	2.874298e-08
8	$[11^{1e}0, 03^{1e}0]_{II}$	5.603843e+13	1.105382e+10	3.987058e+03	3.137187e-03	-2.701216e-08
9	$[11^{1f}0, 03^{1f}0]_I$	6.012168e+13	1.106516e+10	3.244822e+03	2.015959e-03	3.883712e-09
10	$[11^{1f}0, 03^{1f}0]_{II}$	5.603843e+13	1.108061e+10	4.164942e+03	2.403481e-03	1.688037e-08
11	$03^{3e}0$	5.788854e+13	1.109632e+10	3.717367e+03	-3.447207e-03	-1.350229e-08
12	$03^{3f}0$	5.788854e+13	1.109632e+10	3.717197e+03	-2.449162e-03	-2.160185e-08
			0 0 2			
13	0^002	1.351688e+14	1.087058e+10	3.540893e+03	4.097846e-04	6.751723e-09
			1 0 1 + 0 2 1			
14	$[10^01, 02^01]_I$	1.075520e+14	1.094820e+10	3.088172e+03	5.606105e-03	2.224787e-09
15	$[10^01, 02^01]_{II}$	1.046394e+14	1.096735e+10	4.202689e+03	5.662843e-03	-3.725155e-08
16	$02^{2e}1$	1.058201e+14	1.099464e+10	3.587035e+03	-9.133817e-03	1.742922e-08
17	$02^{2f}1$	1.058201e+14	1.099464e+10	3.665833e+03	9.675907e-04	-2.057591e-08

49

Table B.15: Molecular constants for the 738 isotopologue of CO_2 (co2amp #: '11'; HITRAN ID: 'A').

#	Level	G (Hz)	B (Hz)	D (Hz)	H (Hz)	L (Hz)
				Ground state		
	00^00	0.000000e+00	1.070090e+10	3.336429e+03	2.117267e-05	1.442116e-08
				0 1 0		
	$01^{1e}0$	1.920360e+13	1.071209e+10	3.381662e+03	8.482200e-05	1.817743e-08
	$01^{1f}0$	1.920360e+13	1.072816e+10	3.386497e+03	-9.613146e-03	1.621095e-06
				0 0 1		
0	0^001	6.763179e+13	1.061985e+10	3.328566e+03	1.629353e-04	5.193608e-09
				1 0 0 + 0 2 0		
1	$[10^00, 02^00]_I$	3.985595e+13	1.070175e+10	2.874895e+03	3.264921e-03	8.185136e-08
2	$[10^00, 02^00]_{II}$	3.695121e+13	1.070641e+10	3.908353e+03	4.339276e-03	1.249170e-07
3	$02^{2e}0$	3.841755e+13	1.073915e+10	3.451459e+03	-7.855086e-03	-7.391810e-08
4	$02^{2f}0$	3.841755e+13	1.073916e+10	3.447316e+03	-2.504127e-03	5.800843e-07
				0 1 1		
5	$01^{1e}1$	8.648984e+13	1.063181e+10	3.370067e+03	2.561471e-04	7.953695e-09
6	$01^{1f}1$	8.648984e+13	1.064745e+10	3.391076e+03	-4.829163e-03	1.064912e-06
				1 1 0 + 0 3 0		
7	$[11^{1e}0, 03^{1e}0]_I$	5.966249e+13	1.070722e+10	3.139798e+03	-1.015316e-02	8.152701e-06
8	$[11^{1e}0, 03^{1e}0]_{II}$	5.557934e+13	1.071403e+10	3.720610e+03	-8.357787e-03	6.860969e-06
9	$[11^{1f}0, 03^{1f}0]_I$	5.966249e+13	1.073160e+10	3.018549e+03	-3.048363e-02	1.589723e-05
10	$[11^{1f}0, 03^{1f}0]_{II}$	5.557934e+13	1.073849e+10	3.879536e+03	-2.175305e-02	1.118141e-05
11	$03^{3e}0$	5.764160e+13	1.075797e+10	3.515123e+03	5.574211e-03	-2.726061e-06
12	$03^{3f}0$	5.764160e+13	1.075798e+10	3.515890e+03	6.458410e-03	-3.125042e-06
				0 0 2		
13	0^002	-	-	-	-	-
				1 0 1 + 0 2 1		
14	$[10^01, 02^01]_I$	1.068645e+14	1.061939e+10	2.859092e+03	3.538311e-03	5.370825e-08
15	$[10^01, 02^01]_{II}$	1.039876e+14	1.062791e+10	3.922476e+03	5.014599e-03	-1.272138e-08
16	$02^{2e}1$	1.053588e+14	1.065927e+10	3.418964e+03	-7.045723e-03	-1.394816e-07
17	$02^{2f}1$	1.053588e+14	1.065928e+10	3.437025e+03	-1.081578e-03	3.478069e-07

Appendix C

Properties of optical materials

The following expressions and values for linear (n_0) and nonlinear (n_2) refractive indexes and linear absorption (α_0) are used in the program (wavelength λ in the formulas must be expressed in µm):

Air

Refractive index n_0 is calculated using Mathar's model for $\lambda = 7.5$–$14\,\mu\text{m}$ [23]

$n_2 = 3.0 \times 10^{-23}\ \text{m}^2/\text{W}$ at $9.2\,\mu\text{m}$ [24]

AgBr

$n_0 = \sqrt{3.860 + \frac{0.8677\lambda^2}{\lambda^2 - 0.3211^2} + \frac{21.61\lambda^2}{\lambda^2 - 254.2^2}}$ ($\lambda = 0.495$–$12.67\,\mu\text{m}$) [25]

$n_2 = 6.0 \times 10^{-19}\ \text{m}^2/\text{W}$ at $9.2\,\mu\text{m}$ [25]

AgCl

$n_0 = \sqrt{4.00804 + \frac{0.079086}{\lambda^2 - 0.04584} - 0.00085111\lambda^2 - 0.00000019762\lambda^4}$ ($\lambda = 0.578$–$20.6\,\mu\text{m}$) [26]

$n_2 = 4.8 \times 10^{-19}\ \text{m}^2/\text{W}$ at $9.2\,\mu\text{m}$ [25]

BaF$_2$

$n_0 = \sqrt{1.33973 + \frac{0.81070\lambda^2}{\lambda^2 - 0.10065^2} + \frac{0.19652\lambda^2}{\lambda^2 - 29.87^2} + \frac{4.52469\lambda^2}{\lambda^2 - 53.82^2}}$ ($\lambda = 0.15$–$15\,\mu\text{m}$) [27]

$n_2 = 1.7 \times 10^{-20}\ \text{m}^2/\text{W}$ at $9.2\,\mu\text{m}$ [28]

$\alpha_0 = 0.8(e^{1.20(\lambda - 8)} - 1)\ \text{m}^{-1}$ [25]

CdTe

$n_0 = \sqrt{1 + \frac{6.1977889\lambda^2}{\lambda^2 - 0.1005326} + \frac{3.2243821\lambda^2}{\lambda^2 - 5279.518}}$ ($\lambda = 6$–$22\,\mu\text{m}$) [29]

$n_2 = -2.95 \times 10^{-17}\ \text{m}^2/\text{W}$ at $1.06\,\mu\text{m}$ [30]

CsI

$$n_0 = \sqrt{1.27587 + \frac{0.68689\lambda^2}{\lambda^2 - 0.130^2} + \frac{0.26090\lambda^2}{\lambda^2 - 0.147^2} + \frac{0.06256\lambda^2}{\lambda^2 - 0.163^2} + \frac{0.06527\lambda^2}{\lambda^2 - 0.177^2} + \frac{0.14991\lambda^2}{\lambda^2 - 0.185^2} + \frac{0.51818\lambda^2}{\lambda^2 - 0.206^2} + \frac{0.01918\lambda^2}{\lambda^2 - 0.218^2} + \frac{3.38229\lambda^2}{\lambda^2 - 161.29^2}}$$
(λ= 0.25–67 µm) [31]

$n_2 = 1.2 \times 10^{-19}$ m^2/W at 9.2 µm [25]

GaAs

$$n_0 = \sqrt{5.372514 + \frac{5.466742\lambda^2}{\lambda^2 - 0.4431307^2} + \frac{0.02429960\lambda^2}{\lambda^2 - 0.8746453^2} + \frac{1.957522\lambda^2}{\lambda^2 - 36.9166^2}}$$ (λ= 0.97–17 µm) [32]

$n_2 = 7.5 \times 10^{-18}$ m^2/W at 9.2 µm [25]

Ge

$$n_0 = \sqrt{1 + \frac{0.4886331\lambda^2}{\lambda^2 - 1.393959} + \frac{14.5142535\lambda^2}{\lambda^2 - 0.1626427} + \frac{0.0091224\lambda^2}{\lambda^2 - 752.190}}$$ (λ= 2–14 µm) [33]

$n_2 = 4.0 \times 10^{-17}$ m^2/W at 9.2 µm [25]

IRG22 (AMTIR1)

$$n_0 = \sqrt{3.4834 + \frac{2.8203\lambda^2}{\lambda^2 - 0.1352} + \frac{0.9773\lambda^2}{\lambda^2 - 1420.7}}$$ (λ= 0.8–15.5 µm) [34]

$n_2 = 1.4 \times 10^{-18}$ m^2/W at 9.2 µm [25]

IRG24

$$n_0 = \sqrt{3.8965 + \frac{2.9567\lambda^2}{\lambda^2 - 0.1620} + \frac{0.9461\lambda^2}{\lambda^2 - 1939.1}}$$ (λ= 0.8–15.5 µm) [35]

$n_2 = 2.5 \times 10^{-18}$ m^2/W at 9.2 µm [25]

IRG25

$$n_0 = \sqrt{3.7574 + \frac{3.0990\lambda^2}{\lambda^2 - 0.1596} + \frac{1.6660\lambda^2}{\lambda^2 - 2045.5}}$$ (λ= 0.8–15.5 µm) [36]

$n_2 = 2.3 \times 10^{-18}$ m^2/W at 9.2 µm [25]

KBr

$$n_0 = \sqrt{1.39408 + \frac{0.79221\lambda^2}{\lambda^2 - 0.146^2} + \frac{0.01981\lambda^2}{\lambda^2 - 0.173^2} + \frac{0.15587\lambda^2}{\lambda^2 - 0.187^2} + \frac{0.17673\lambda^2}{\lambda^2 - 60.61^2} + \frac{2.06217\lambda^2}{\lambda^2 - 87.72^2}}$$ (λ= 0.2–42 µm) [31]

$n_2 = 4.3 \times 10^{-20}$ m^2/W at 9.2 µm [25]

KCl

$$n_0 = \sqrt{1.26486 + \frac{0.30523\lambda^2}{\lambda^2 - 0.100^2} + \frac{0.41620\lambda^2}{\lambda^2 - 0.131^2} + \frac{0.18870\lambda^2}{\lambda^2 - 0.162^2} + \frac{2.6200\lambda^2}{\lambda^2 - 70.42^2}}$$ (λ= 0.18–35 µm) [31]

$n_2 = 3.4 \times 10^{-20}$ m^2/W at 9.2 µm [28]

KRS5

$n_0 = \sqrt{1 + \frac{1.8293958\lambda^2}{\lambda^2 - 0.0225} + \frac{1.6675593\lambda^2}{\lambda^2 - 0.0625} + \frac{1.1210424\lambda^2}{\lambda^2 - 0.1225} + \frac{0.04513366\lambda^2}{\lambda^2 - 0.2025} + \frac{12.380234\lambda^2}{\lambda^2 - 27089.737}}$ ($\lambda = 0.577$–$39.4\,\mu m$) [37]

$n_2 = 9.0 \times 10^{-19}\ m^2/W$ at $9.2\,\mu m$ [25]

NaCl

$n_0 = \sqrt{1.00055 + \frac{0.19800\lambda^2}{\lambda^2 - 0.050^2} + \frac{0.48398\lambda^2}{\lambda^2 - 0.100^2} + \frac{0.38696\lambda^2}{\lambda^2 - 0.128^2} + \frac{0.25998\lambda^2}{\lambda^2 - 0.158^2} + \frac{0.08796\lambda^2}{\lambda^2 - 40.50^2} + \frac{3.17064\lambda^2}{\lambda^2 - 60.98^2} + \frac{0.30038\lambda^2}{\lambda^2 - 120.34^2}}$ ($\lambda = 0.2$–$30\,\mu m$) [31]

$n_2 = 3.5 \times 10^{-20}\ m^2/W$ at $9.2\,\mu m$ [28]

NaF

$n_0 = \sqrt{1.41572 + \frac{0.32785\lambda^2}{\lambda^2 - 0.117^2} + \frac{3.18248\lambda^2}{\lambda^2 - 40.57^2}}$ ($\lambda = 0.15$–$17\,\mu m$) [31]

$n_2 = 6.0 \times 10^{-21}\ m^2/W$ at $9.2\,\mu m$ at $9.2\,\mu m$ [25]

$\alpha_0 = 5.0(e^{0.97(\lambda - 8)} - 1)\ m^{-1}$ [25]

Si

$n_0 = 3.41983 + \frac{0.159906}{\lambda^2 - 0.028} - 0.123109\left(\frac{1}{\lambda^2 - 0.028}\right)^2 + 1.26878 \times 10^{-6}\lambda^2 - 1.95104 \times 10^{-9}\lambda^4$ ($\lambda = 2.44$–$25\,\mu m$) [38]

$n_2 = 1.2 \times 10^{-17}\ m^2/W$ at $9.2\,\mu m$ [25]

SiO$_2$

$n_0 = \sqrt{1 + \frac{0.6961663\lambda^2}{\lambda^2 - 0.0684043^2} + \frac{0.4079426\lambda^2}{\lambda^2 - 0.1162414^2} + \frac{0.8974794\lambda^2}{\lambda^2 - 9.896161^2}}$ ($\lambda = 0.21$–$6.7\,\mu m$) [39]

$n_2 = 3.29 \times 10^{-20}\ m^2/W$ at $1.06\,\mu m$ [30]

ZnS

$n_0 = \sqrt{8.393 + \frac{0.14383}{\lambda^2 - 0.2421^2} + \frac{4430.99}{\lambda^2 - 36.71^2}}$ ($\lambda = 0.405$–$13\,\mu m$) [40]

$n_2 = 4.0 \times 10^{-19}\ m^2/W$ at $9.2\,\mu m$ [25]

ZnSe

$n_0 = \sqrt{1 + \frac{4.45813734\lambda^2}{\lambda^2 - 0.200859853^2} + \frac{0.467216334\lambda^2}{\lambda^2 - 0.391371166^2} + \frac{2.89566290\lambda^2}{\lambda^2 - 47.1362108^2}}$ ($\lambda = 0.54$–$18.2\,\mu m$) [41]

$n_2 = 6.5 \times 10^{-19}\ m^2/W$ at $9.2\,\mu m$ [25]

Appendix D

Selected formulas explained

Equation 4.10

Eq. 4.10 defines the fraction z_{jk} of discharge energy spent in inelastic collisions:

$$z_{jk} = 10^{16} \frac{y_j u_{jk} \omega_{jk}}{\left(\frac{\xi \mathcal{E}}{\mathcal{N}}\right) v_d}$$

where $y_j[-]$ is the relative concentration of a component in the gas mixture, $u_{jk}[\text{eV}]$ is the transferred energy per electron-molecule collision, collision rate constant $\omega_{jk}[\text{cm}^3 \cdot \text{s}^{-1}]$ divided by electron drift speed $v_d[\text{cm} \cdot \text{s}^{-1}]$ is the collision cross-section ($[\text{cm}^2]$), $\mathcal{E}[10^{-16}\text{V} \cdot \text{cm}^{-1}]$ is the electric field, $\xi[\text{eV} \cdot \text{V}^{-1}]$ is the energy gained by electron moved across an electric potential difference of 1 V, and $\mathcal{N}[\text{cm}^{-3}]$ is the total absolute concentration of the gas mixture.

The physical meaning of $\xi \mathcal{E}$ is the energy (in eV) gained by an electron after passing 1 cm in the electric field $\mathcal{E}$. By definition of electronvolt, $\xi = 1$ and is thus omitted in Eq. 4.10.

Pumping rate constants in equations 4.13

Pumping rate constant is the number of quanta added to a given vibrational mode per unit of time per molecule.

$$p_e = \frac{1}{E_v[\text{J}]} \times \frac{1}{N[\text{cm}^{-3}]n[-]y[-]} \times q[-]W[\text{J} \cdot \text{s}^{-1} \cdot \text{cm}^{-3}]$$

where E_v is the energy of the vibrational quanta: 4.665e-20 J (2349 cm^{-1}) for ν_3 mode of CO_2 (and roughly same for N_2 vibration), and 1.325e-20 J (667 cm^{-1}) for ν_2 mode; N=2.7e19 cm^{-3} is the density of gas molecules under normal conditions (1 bar, 273 K); q is the fraction of discharge energy deposited in the corresponding vibration; n is the correction factor for molecular density at the conditions different from 'normal'; y is the relative concentration of the gas in the mixture; W is the discharge power density.

Combining the constants and switching to kW/cm^3 for power density and μs^{-1} for the rate constants we get the formulas given in the model description:

$$p_{e4} = 0.8 \times 10^{-3} \frac{q_4}{ny_2} W(t); \quad p_{e3} = 0.8 \times 10^{-3} \frac{q_3}{ny_1} W(t); \quad p_{e2} = 2.8 \times 10^{-3} \frac{q_2}{ny_1} W(t);$$

Solution of Boltzmann equation 4.7

To find the distribution function $f(u)$ from Eq. 4.7, we first represent the equation in the following discrete form.

$$\frac{1}{3}\left(\frac{\mathcal{E}}{\mathcal{N}}\right)^2\frac{1}{2du}\left[u_{i+1}\left(\sum_j y_j Q_{mj}(u_{i+1})\right)^{-1}\frac{f_{i+2}-f_i}{2du}-u_{i-1}\left(\sum_j y_j Q_{mj}(u_{i-1})\right)^{-1}\frac{f_i-f_{i-2}}{2du}\right]$$

$$+1.09\times10^{-3}\frac{1}{2du}\left[u_{i+1}^2 f_{i+1}\sum_j\frac{y_j}{M_j}Q_{mj}(u_{i+1})-u_{i-1}^2 f_{i-1}\sum_j\frac{y_j}{M_j}Q_{mj}(u_{i-1})\right]$$

$$+\sum_{j=1,2}y_j C_j\frac{u_{i+1}f_{i+1}-u_{i-1}f_{i-1}}{2du}+6By_2\frac{u_{i+1}Q(u_{i+1})f_{i+1}-u_{i-1}Q(u_{i-1})f_{i-1}}{2du}\,(uQ(u)f)$$

$$+\sum_j y_j\sum_k(u_i+u_{jk})Q_{jk}(u_i+u_{jk})f_x-u_if_i\sum_j y_j\sum_k Q_{jk}(u_i)=0,$$

where du is the grid step, $u_i=i\times du$, $f_i=f(u_i)$, and $f_x=f(i+u_{jk}/du)$. We use 1024 steps in the grid $i=0...1023$.

We now have a system of 1024 equations for 1024 values of f_i corresponding to the values of u_i. The coefficients of the equations are summarized below.

$\mathbf{f_i}$:

$$-\sum_j y_j\sum_k u_i Q_{jk}(u_i)-$$

$$-\frac{1}{3}\left(\frac{\mathcal{E}}{\mathcal{N}}\right)^2\frac{1}{4(du)^2}\left[u_{i+1}\left(\sum_j y_j Q_{mj}(u_{i+1})\right)^{-1}-u_{i-1}\left(\sum_j y_j Q_{mj}(u_{i-1})\right)^{-1}\right]$$

$\mathbf{f_{i+u_{jk}/du}}$:

$$y_j(u_i+u_{jk})Q_{jk}(u_i+u_{jk})$$

$\mathbf{f_{i+1}}$:

$$1.09\times10^{-3}\frac{1}{2du}u_{i+1}^2 f_{i+1}\sum_j\frac{y_j}{M_j}Q_{mj}(u_{i+1})+\sum_{j=1,2}y_j C_j\frac{u_{i+1}}{2du}+6By_2\frac{u_{i+1}Q(u_{i+1})}{2du}$$

$\mathbf{f_{i-1}}$:

$$-1.09\times10^{-3}\frac{1}{2du}u_{i-1}^2 f_{i-1}\sum_j\frac{y_j}{M_j}Q_{mj}(u_{i-1})-\sum_{j=1,2}y_j C_j\frac{u_{i-1}}{2du}-6By_2\frac{u_{i-1}Q(u_{i-1})}{2du}$$

$\mathbf{f_{i+2}}$:

$$\frac{1}{3}\left(\frac{\mathcal{E}}{\mathcal{N}}\right)^2\frac{1}{4(du)^2}u_{i+1}\left(\sum_j y_j Q_{mj}(u_{i+1})\right)^{-1}$$

$\mathbf{f_{i-2}}$:

$$\frac{1}{3}\left(\frac{\mathcal{E}}{\mathcal{N}}\right)^2\frac{1}{4(du)^2}u_{i-1}\left(\sum_j y_j Q_{mj}(u_{i-1})\right)^{-1}$$

These equations are then solved using the tridiagonal matrix algorithm.

Bibliography

[1] M. Born and E. Wolf, *Principles of Optics: Electromagnetic Theory of Propagation, Interference and Diffraction of Light*. Cambridge University Press, 1999.

[2] A. E. Siegman, *Lasers*. University Science Books, 1986.

[3] J. Peatross and M. Ware, *Physics of Light and Optics*. Available at optics.byu.edu, 2015.

[4] I. Gordon *et al.*, "The hitran2020 molecular spectroscopic database," *Journal of Quantitative Spectroscopy and Radiative Transfer*, vol. 277, p. 107 949, 2022, ISSN: 0022-4073. DOI: 10.1016/j.jqsrt.2021.107949.

[5] W. J. Witteman, *The CO_2 Laser*. Berlin Heidelberg New York Tokyo: Springer-Verlag, 1987.

[6] J. Finzi and C. B. Moore, "Relaxation of $CO_2(10^01)$, $CO_2(02^01)$, and $N_2O(10^01)$ vibrational levels by near-resonant V→V energy transfer," *J. Chem. Phys.*, vol. 63, pp. 2285–2288, 1975. DOI: 10.1063/1.431678.

[7] N. V. Karlov and Y. B. Konev, "High pressure pulsed CO_2 lasers," in *Handbook on lasers*, A. M. Prokhorov, Ed., In Russian, Moscow: Sovetskoe Radio, 1978.

[8] T. Holstein, "Energy distribution of electrons in high frequency gas discharges," *Phys. Rev.*, vol. 70, pp. 367–384, 1946. DOI: 10.1103/PhysRev.70.367.

[9] W. L. Nighan, "Electron energy distributions and collision rates in electrically excited N_2, CO, and CO_2," *Phys. Rev. A*, vol. 2, pp. 1989–2000, 1970. DOI: 10.1103/PhysRevA.2.1989.

[10] R. D. Hake and A. V. Phelps, "Momentum-transfer and inelastic-collision cross sections for electrons in O_2, CO, and CO_2," *Phys. Rev.*, vol. 158, pp. 70–84, 1967. DOI: 10.1103/PhysRev.158.70.

[11] L. S. Frost and A. V. Phelps, "Rotational excitation and momentum transfer cross sections for electrons in H_2 and N_2 from transport coefficients," *Phys. Rev.*, vol. 127, pp. 1621–1633, 1962. DOI: 10.1103/PhysRev.127.1621.

[12] A. S. Biryukov, V. K. Konyukhov, A. I. Lukovnikov, and R. I. Serikov, "Relaxation of the vibrational energy of the (00^01) level of the CO_2 molecule," *Sov. J. Exp. Theor. Phys.*, vol. 39, p. 610, 1974.

[13] R. L. Taylor and S. Bitterman, "Survey of vibrational relaxation data for processes important in the CO_2-N_2 laser system," *Rev. Mod. Phys.*, vol. 41, pp. 26–47, 1969. DOI: 10.1103/RevModPhys.41.26.

[14] B. J. Feldman, "Short-pulse multiline and multiband energy extraction in high-pressure CO_2-laser amplifiers," *IEEE J. Quant. Electron.*, vol. 9, pp. 1070–1078, 1973. DOI: 10.1109/JQE.1973.1077412.

[15] H. C. Volkin, "Calculation of short-pulse propagation in a large CO_2-laser amplifier," *J. Appl. Phys.*, vol. 50, pp. 1179–1188, 1979. DOI: 10.1063/1.326148.

[16] R. C. Hilborn, "Einstein coefficients, cross sections, f values, dipole moments, and all that," *arXiv:physics/0202029*, 2002.

[17] J. J. Lowke, A. V. Phelps, and B. W. Irwin, "Predicted electron transport coefficients and operating characteristics of CO_2-N_2-He laser mixtures," *J. Appl. Phys.*, vol. 44, pp. 4664–4671, 1973. DOI: 10.1063/1.1662017.

[18] Y. D. Oksyuk, "Excitation of the rotational levels of diatomic molecules by electron impact in the adiabatic approximation," *Sov. J. Exp. Theor. Phys.*, vol. 22, pp. 873–881, 1966.

[19] N. Chandra and P. G. Burke, "Rotational excitation cross sections for e$^-$-N$_2$ scattering," *J. Phys. B: At. Mol. Phys.*, vol. 6, pp. 2355–2357, 1973. DOI: 10.1088/0022-3700/6/11/030.

[20] A. V. Phelps, "Rotational and vibrational excitation of molecules by low-energy electrons," *Rev. Mod. Phys.*, vol. 40, pp. 399–410, 1968. DOI: 10.1103/RevModPhys.40.399.

[21] G. J. Schulz, "Vibrational excitation of nitrogen by electron impact," *Phys. Rev.*, vol. 125, pp. 229–232, 1962. DOI: 10.1103/PhysRev.125.229.

[22] A. G. Engelhardt, A. V. Phelps, and C. G. Risk, "Determination of momentum transfer and inelastic collision cross sections for electrons in nitrogen using transport coefficients," *Phys. Rev.*, vol. 135, A1566–A1574, 1964. DOI: 10.1103/PhysRev.135.A1566.

[23] R. J. Mathar, "Refractive index of humid air in the infrared: Model fits," *J. Opt. A*, vol. 9, pp. 470–476, 2007. DOI: 10.1088/1464-4258/9/5/008.

[24] M. N. Polyanskiy, M. Babzien, I. V. Pogorelsky, R. Kupfer, K. L. Vodopyanov, and M. A. Palmer, "Single-shot measurement of the nonlinear refractive index of air at 92 μm with a picosecond terawatt CO$_2$ laser," *Opt. Lett.*, vol. 46, p. 2067, 2021. DOI: 10.1364/ol.423800.

[25] M. N. Polyanskiy, I. V. Pogorelsky, M. Babzien, K. L. Vodopyanov, and M. A. Palmer, "Nonlinear refraction and absorption properties of optical materials for high-peak-power long-wave-infrared lasers," *Optical Materials Express*, vol. 14, p. 696, 2024. DOI: 10.1364/ome.513971.

[26] L. W. Tilton, E. K. Plyler, and R. E. Stephens, "Refractive index of silver chloride for visible and infra-red radiant energy," *J. Opt. Soc. Am.*, vol. 40, p. 540, 1950. DOI: 10.1364/josa.40.000540.

[27] H. H. Li, "Refractive index of alkaline earth halides and its wavelength and temperature derivatives," *J. Phys. Chem. Ref. Data*, vol. 9, pp. 161–290, 1980. DOI: 10.1063/1.555616.

[28] M. N. Polyanskiy, I. V. Pogorelsky, M. Babzien, R. Kupfer, K. L. Vodopyanov, and M. A. Palmer, "Post-compression of long-wave infrared 2 picosecond sub-terawatt pulses in bulk materials," *Opt. Express*, vol. 29, p. 31 714, 2021. DOI: 10.1364/oe.434238.

[29] A. G. DeBell, E. L. Dereniak, J. Harvey, J. P. J. Nissley, A. Selvarajan, and W. L. Wolfe, "Cryogenic refractive indices and temperature coefficients of cadmium telluride from 6 μm to 22 μm," *Appl. Opt.*, vol. 18, pp. 3114–3115, 1979. DOI: 10.1364/AO.18.003114.

[30] M. Sheik-Bahae, "Dispersion of bound electron nonlinear refraction in solids," *IEEE J. Quant. Electron.*, vol. 27, pp. 1296–1309, 1991. DOI: 10.1109/3.89946.

[31] H. H. Li, "Refractive index of alkali halides and its wavelength and temperature derivatives," *J. Phys. Chem. Ref. Data*, vol. 5, pp. 329–528, 1976. DOI: 10.1063/1.555536.

[32] T. Skauli *et al.*, "Improved dispersion relations for GaAs and applications to nonlinear optics," *J. Appl. Opt.*, vol. 94, pp. 6447–6455, 2003. DOI: 10.1063/1.1621740.

[33] J. H. Burnett, S. G. Kaplan, E. Stover, and A. Phenis, "Refractive index measurements of ge," P. D. LeVan, A. K. Sood, P. Wijewarnasuriya, and A. I. D'Souza, Eds., SPIE Optical Engineering + Applications, 2016, San Diego, California, United States, SPIE, 2016. DOI: 10.1117/12.2237978.

[34] *SCHOTT IRG 22 product flyer*, Apr. 2017. [Online]. Available: https://refractiveindex.info/download/data/2017/schott-infrared-chalcogenide-glasses-irg-22-english-us-11052017.pdf.

[35] *SCHOTT IRG 24 product flyer*, Apr. 2017. [Online]. Available: https://refractiveindex.info/download/data/2017/schott-infrared-chalcogenide-glasses-irg-24-english-us-10042017.pdf.

[36] *SCHOTT IRG 25 product flyer*, Apr. 2017. [Online]. Available: https://refractiveindex.info/download/data/2017/schott-infrared-chalcogenide-glasses-irg-25-english-us-10042017.pdf.

[37] W. S. Rodney and I. H. Malitson, "Refraction and dispersion of thallium bromide iodide," *Journal of the Optical Society of America*, vol. 46, p. 956, 1956. DOI: 10.1364/josa.46.000956.

[38] D. F. Edwards and E. Ochoa, "Infrared refractive index of silicon," *Appl. Opt.*, vol. 19, pp. 4130–4131, 1980. DOI: 10.1364/AO.19.004130.

[39] I. H. Malitson, "Interspecimen comparison of the refractive index of fused silica," *J. Opt. Soc. Am.*, vol. 55, p. 1205, 1965. DOI: 10.1364/josa.55.001205.

[40] C. A. Klein, "Room-temperature dispersion equations for cubic zinc sulfide," *Appl. Opt.*, vol. 25, p. 1873, 1986. DOI: 10.1364/ao.25.001873.

[41] B. Tatian, "Fitting refractive-index data with the Sellmeier dispersion formula," *Appl. Opt.*, vol. 23, pp. 4477–4485, 1984. DOI: 10.1364/AO.23.004477.